NASA CR-
160458

(NASA-CR-160458) A GROUND BASED PHASE CONTROL SYSTEM FOR THE SOLAR POWER SATELLITE, VOLUME 4 Final Report (LinCom Corp., Pasadena, Calif.) 66 p HC A04/MF A01 CSCL 22B G3/15

N80-17123

Unclas
47118

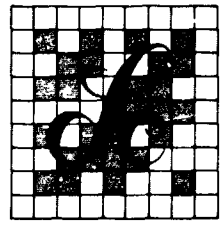

LinCom Corporation
PO Box 2793D, Pasadena, Calif 91105

LinCom

FINAL REPORT

PHASE III

A GROUND BASED PHASE CONTROL SYSTEM FOR THE SOLAR POWER SATELLITE

VOLUME IV

PREPARED FOR

NASA JOHNSON SPACE CENTER
HOUSTON, TX 77058

TECHNICAL MONITOR: JACK SEYL

CONTRACT NO. NAS9-15782

PREPARED BY

C. M. CHIE

LINCOM CORPORATION
P.O. BOX 2793D
PASADENA, CA 91105

JANUARY 1980

TR-0180-0779

LinCom

TABLE OF CONTENTS

TABLE OF CONTENTS (Cont'd)

SUMMARY

In this report, a ground-based phase control system is studied as an alternative approach to the current reference retrodirective phase control system. The ground-based concept is anticipated to simplify the spaceborne hardware requirement.

The implementation of the ground-based phase control concept is determined mainly by the phase control waveform designs employed. In the ground based phase control system, three different waveforms are required in the design: (1) downlink frequency reference signal, (2) downlink subarray (power module) transmission and (3) a uplink phase error correction command signal. Based on our waveform selections, functional subsystems to implement the ground-based phase control concept are identified and functionally represented. The resultant ground-based phase control system includes:

- Satellite Signal Processing
  - Time-Frequency Control
  - Processing Control Center
  - Signal Distribution Network
  - Processing Power Module
  - Downlink Pilot Transmitter
  - Uplink Command Receiver
- Ground Based Signal Processing
  - Pilot Beacon Receiver
  - Calibration Receiver
  - Phase Measurement Unit

- Synchronization Unit
- Phase Update Algorithm
- Data Processing Unit
- Uplink Command Transmitter

The associated initial start-up procedure is also considered.

The ground-based system envisioned employs satellite based frequency/timing reference with an IF frequency of 490 MHz. A 4-tone measurement scheme using frequencies at 2,450 $\pm$ 9.57 MHz and 2,450 $\pm$ 19.14 MHz is selected. Each power module devotes 10 μsec per second for phase correction measurement, representing a minimal loss in total power transmitted. Two frequencies are chosen for the downlink and one frequency for the uplink; the downlink pilot signal center frequency is set at 4.9 GHz.

Our preliminary investigation indicates that the effects of power beam interference and thermal noise on the phase measurement error can be limited to a tolerable level. The ground based system can also function if the ionosphere is nonturbulent in nature and the satellite's tilt rate is limited to 0.5 $\widehat{\text{min}}$/sec. The feasibility of the ground-based phase control concept becomes unclear if the conditions on the ionosphere and the satellite motion are not met. At this point, we feel that the development and specification of models for ionospheric phase disturbance and satellite motion is essential.

Further efforts for the ground-based phase control study should be directed towards:

(1) Development of detailed subsystem analytical model.

(2) Tradeoffs for waveform designs.

(3) Development of computer simulation/graphics capabilities for performance analysis and system evaluations and tradeoffs.

(4) Study of satellite data distribution system networking methodology.

(5) Detailed comparison with the retrodirective reference system.

Finally, the hybrid phase control system concept deserves to be investigated as it appears to overcome certain shortcomings of the reference retrodirective and the ground-based phase control system.

1.0 INTRODUCTION

The NASA/DOE Solar Power Satellite (SPS) Concept, under study since it was first suggested by Glaser [1], envisions several hundred thousand synchronized microwave power amplifiers operating in parallel to produce an aggregate power output of 5-10 GW. This power is to be transmitted to the Earth using a microwave/millimeter-wave beaming system operating in a synchronous orbit.

There are two basic elements required in the operation of a SPS. They are the transmitting antenna, hereafter called the spacetenna, and the receiving rectifier antenna, hereafter called the rectenna. The purpose of the spaceborne 1 Km diameter spacetenna is to point and focus the phase coherent microwave beam to a ground-based rectenna which is approximately 10 Km in diameter. The function of beam pointing and focusing is performed by a Phase Control System on board the SPS. Fig.1.1 illustrates the path of the microwave beam from SPS. The distance in the figure are drawn approximately to scale so as to reveal the spatial geometry defined by the SPS microwave power transmission system.

Efficient transmission of the microwave power from the spacetenna to the rectenna is predicated on the ability to accurately focus and point the power beam. Unfortunately, such an ability has never been demonstrated previously in this scale nor has there been such a necessity to do so. As such, different phase control concepts must be continuously updated, compared and evaluated as the SPS program evolves, at least on the system engineering level. In the current reference baseline for the phase control system, the spacetenna is an active retrodirective phased-array: a pilot signal transmitted from the center of the rectenna is phase conjugated at each power

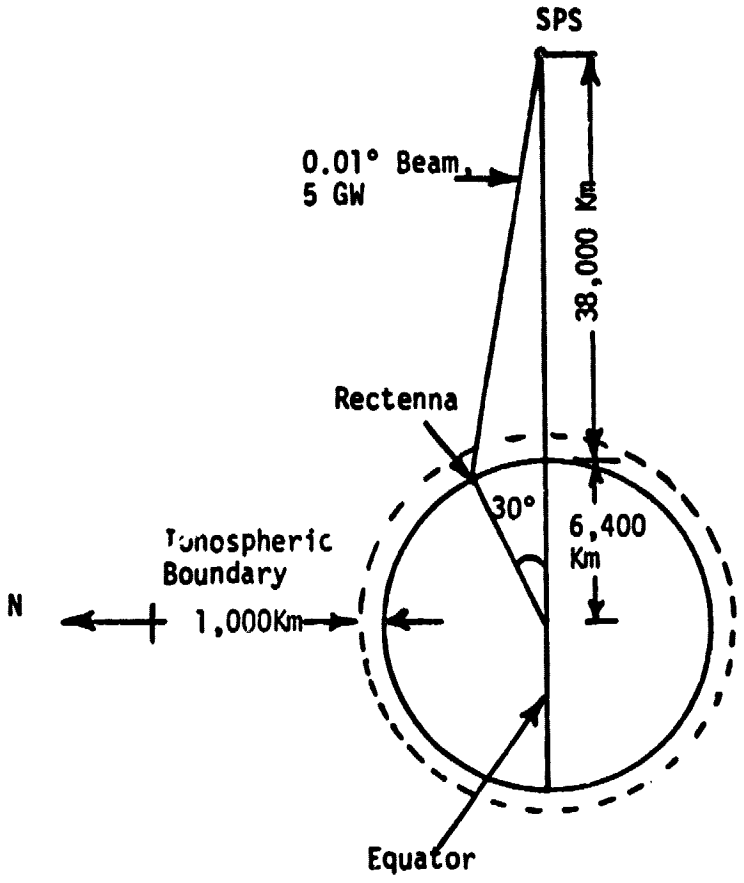

Figure 1.1. Path of Microwave Beam from Solar Power Satellite (SPS).

module [1]. The system can be partitioned into three levels. The first level consists of a reference phase distribution tree which electronically compensates for distribution path length variations to maintain a constant phase reference at each power module. The second level consists of 101,552 power transponders which receive a NRZ/BPSK/BI- -DS signal, allowing reconstruction of a phantom carrier at the same frequency of the power beam. The third level of control is associated with maintaining an equal and constant phase shift through the klystron amplifier at each and every power module. The overall system requires a large amount of spaceborne electronic circuitry on the spacetenna. This is true in particular for the phase reference distribution system.

In this report, a ground-based phase control concept modeled after work done by the NOVAR Corporation and expanded on by Dr. J. Vanelli of LEC is evaluated in terms of its feasibility and implementation at the system engineering level. The main impetus behind this a-proach is to reduce the amount of spaceborne hardware required. Since the beam forming is accomplished by ground command, inherent protection against beam stealing and intentional interference of the system operation is provided. The ground-based phase control system achieves beam forming by adjusting the phases of the individual transmitters on board SPS. The phase adjustments are controlled by ground commands. To specify the correct amount of adjustments, the phases of the power beams from each individual transmitter arriving at the rectenna center must be measured, the appropriate corrections determined (to insure that all power beams arrive at the same phase) and relayed to the SPS. The proposed scheme to be considered in

this report is sequential in nature, i.e., the phase measurement is performed one at a time for each individual transmitter at approximately one second intervals (measurement time allocated is 10 μsec). The phase corrections are updated once every second. A 10-bit phase quantization for the corrections giving 0.35° resolution is envisioned. The uplink command data rate is on the order of 10 Mbps. The functional operation of the ground-based phase control concept is summarized in Fig. 1.2. As evident from the figure, the key issues that need to be studied are:

(1) measurement waveform design and selection,

(2) phase measurement pilot reference design and selection,

(3) uplink phase corrections command link format and design, and

(4) system synchronization techniques.

We start out by quantifying analytically the different aspects of the SPS channel which are of importance to the proper design of the ground-based phase control system. They include the satellite motion, the effect of the ionosphere, thermal noise and interference from the downlink power beam. In the next section, we describe the functional requirements for the ground-based phase control system. Various approaches to achieve these functions will be considered. In many cases, we formulate preliminary mathematical models from which performance can be subsequently

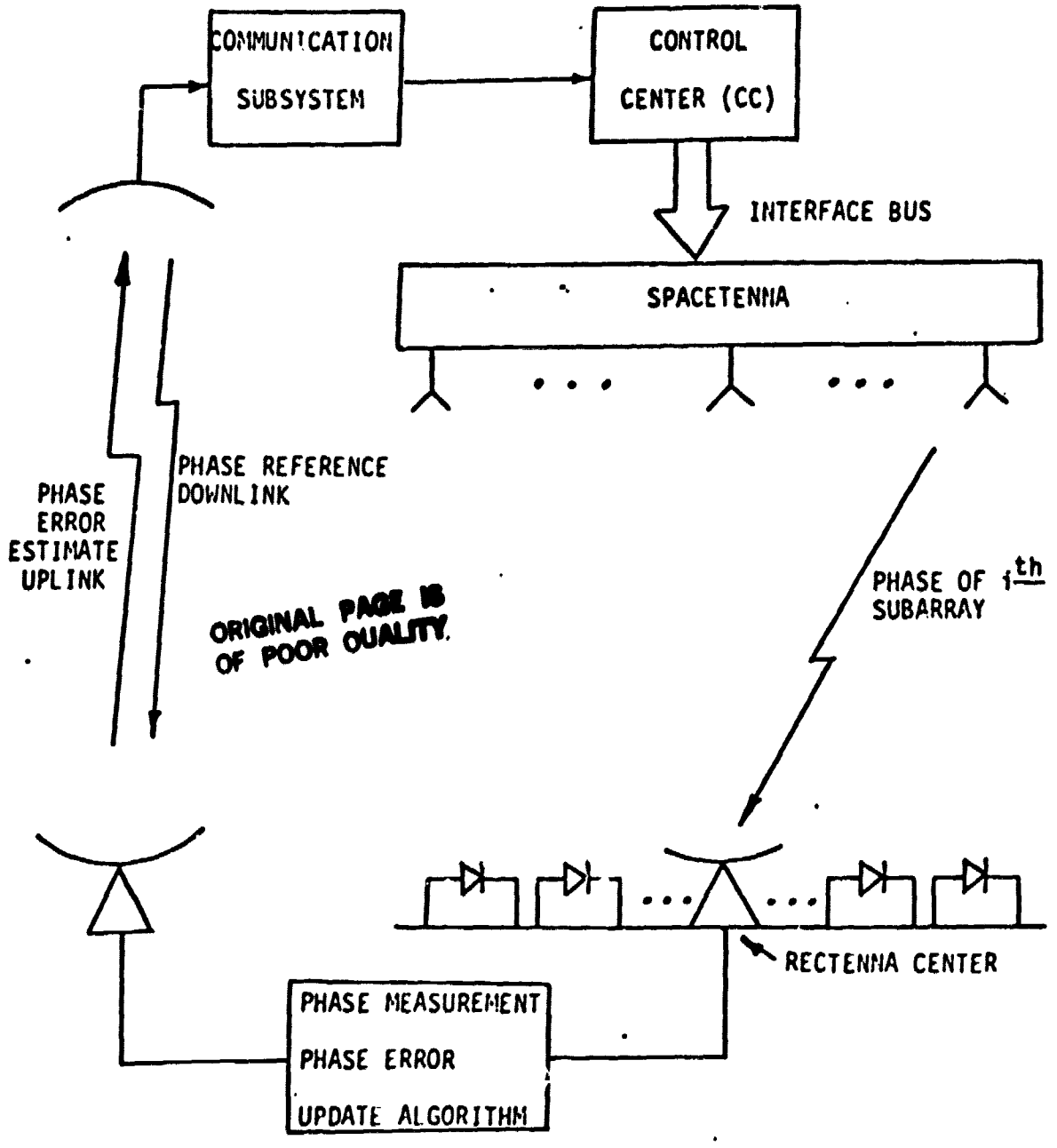

Figure 1.2. Ground Based Phase Control System Concept with Major Functional Blocks.

80 0056

determined. In the last section, a baseline SPS ground-based phase control system is proposed. Its design is sufficiently complete in detail to enable further critique and performance analysis. The salient features of the propcsed baseline system is iisted in Fig. 1.3. For illustrative purposes, these features are contrasted with the Retrofire Reference system.

The feasibility of a ground based phase control system depends on many factors, of which most can be overcome with a proper design, but a few of them are not readily amenable to any cost effective solutions. These are the limiting factors that determine the efficiency of the microwave power transmission system. One of them is the phase fluctuations on the individual microwave beam induced by the ionosphere. As indicated in Fig. 1.3, the ground based phase control system can only correct for random phase fluctuations which have a correlation time that is large compared with 1.25 sec. The noise components which are faster than 1.25 sec is uncompensated for and result in a degradation on transmission efficiency. Unfortunately, measured ionosphere data which is suitable for the SPS system is not readily available. (Most data are concerned with spatial correlations rather than temporal correlations. Also, most data are measured from low orbit satellites rather than geostationary satellites). The other limiting factor is the statistical behavior of the random pointing error exhibited by the spacetenna. Again, the fast component of this error is not corrected for and it contributes to efficiency degradation. It is our hope that the findings of the present report can serve as a guideline for any parallel efforts in studying these two factors.

There are other factors that serve as drivers to determine the performance of the ground based phase control system. They depend

REFERENCE SYSTEM	GROUND BASED SYSTEM
•REQUIRES LARGE AMOUNT OF SPACEBORNE ELECTRONICS	•REQUIRES LESS SPACEBORNE ELECTRONICS
•COMPLEX SPACEBORNE PROCESSING BUT SIMPLE GROUND SIGNAL PROCESSING	•COMPLEX GROUND PROCESSING BUT SIMPLE SPACEBORNE SIGNAL PROCESSING
•CORRECTS FOR IONOSPHERIC DISTURBANCES WITH CORRELATION TIME MORE THAN 0.25 sec	•CORRECTS FOR IONOSPHERIC DISTURBANCES WITH CORRELATION TIME MORE THAN 1.25 sec
•REQUIRES PN CODE FOR SECURITY	•SECURITY OF DOWNLINK
•INSTANTANEOUS CORRECTION FOR SPACETENNA MOTION	•SENSITIVE TO RATE OF CHANGE OF POINTING ERROR
•PERFORMANCE INHERENTLY LIMITED BY THE PHASE ERROR INTRODUCED BY THE PHASE REFERENCE DISTRIBUTION SYSTEM	•PERFORMANCE INHERENTLY LIMITED BY PHASE ERROR INTRODUCED BY THE DIGITAL PHASE SHIFTER
•DOES NOT CORRECT FOR DC PHASE OFFSETS BEYOND THE PHASE CONJUGATION POINT	•NOT AFFECTED BY DC OFFSETS INTRODUCED ANYWHERE ALONG THE SIGNAL PATH
•FAST START-UP	•SLOWER START-UP

Figure 1.3. Salient Features of the Ground Based Phase Control System and Their Comparison to the Reference Baseline System.

80 0057

on projected technologies, e.g., the availability of low noise S-band ten bit digital phase shifters, and low noise, wide band (40 MHz) klystrons. Additional effort is also required in designing an effective, synchronous data distribution network for the reference IF signal, monitor and control commands, and phase correction commands on board the SPS.

2.0 SPS GROUND BASED PHASE CONTROL CHANNEL MODEL

The key elements of the SPS ground based phase control channel are indicated in Fig. 2.1. They include:

(1) Instantaneous range variations due to the motion of the satellite.

(2) Ionospheric effects.

(3) Receiver thermal noise.

(4) Interference from the downlink power beam.

In what follows, we shall examine these elements in terms of their impact on the SPS ground control concept at the system engineering level. The tentative choice of our baseline system will be determined by its ability to overcome these constraints.

2.1 Satellite Motion

The SPS satellite will be in an elliptical orbit with an eccentricity of approxomately 10^{-3} and a mean orbit radius of 42,164 Km [2]. The path of the satellite relative to a satellite in circular synchronous orbit is depicted in Fig. 2.2. Relative to a fixed point on Earth, i.e., the rectenna, the range of the satellite is changing continuously as a function of time. This range variation has a period of 24 hrs. The radial velocity of the satellite relative to the rectenna as a function of the time from perigee is plotted in Fig. 2.3 [2]. It is zero at perigee and takes its maximum value of 307.5 cm/s at 6 hrs from perigee. From Fig. 2.3, it is estimated that the maximum acceleration is .02 cm/s^2.

To assess the impact of this motion on the performance of the ground-based phase control system, we need to investigate the SPS

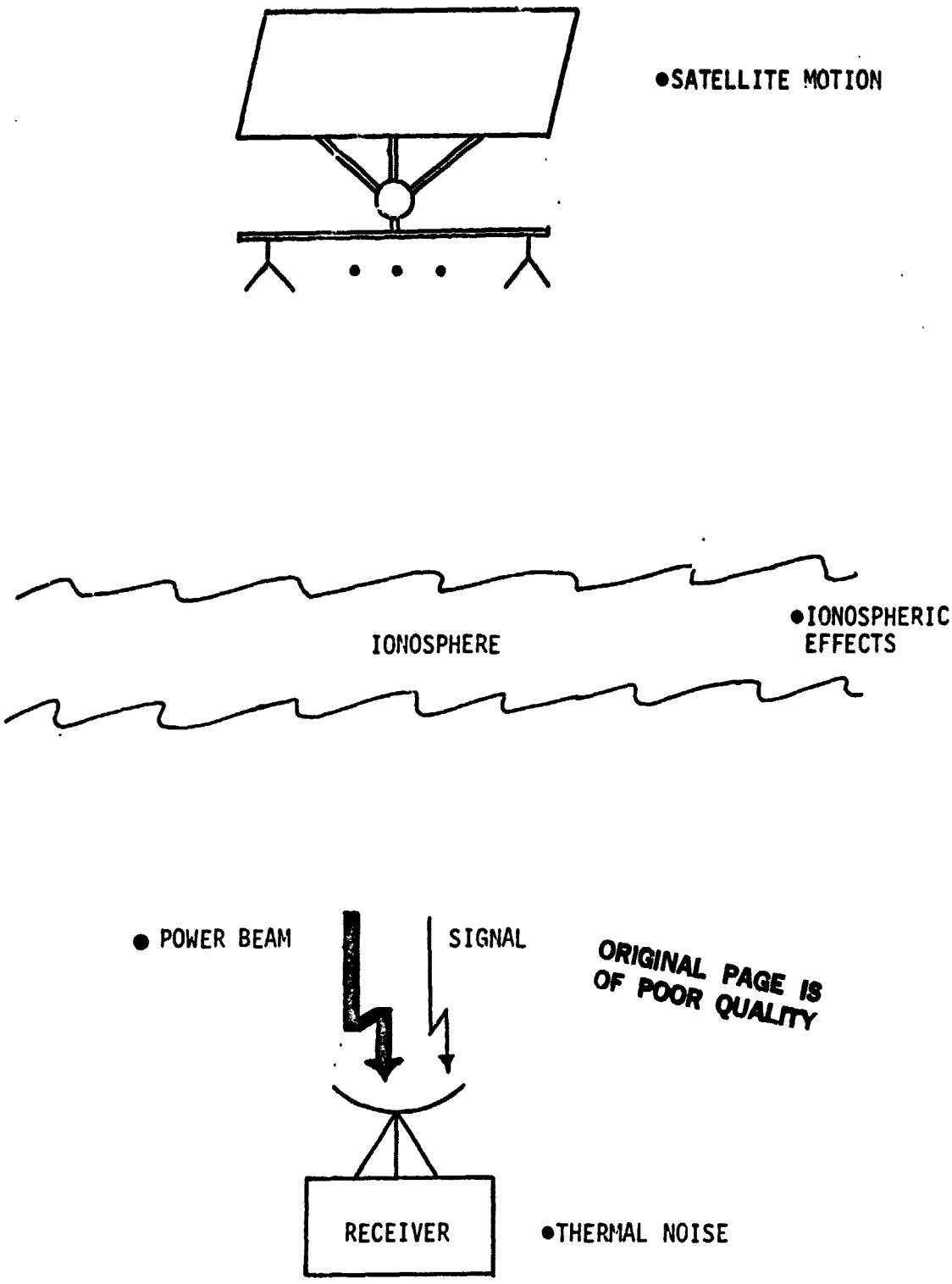

Figure 2.1. Salient Characteristics of SPS Ground Control Channel.

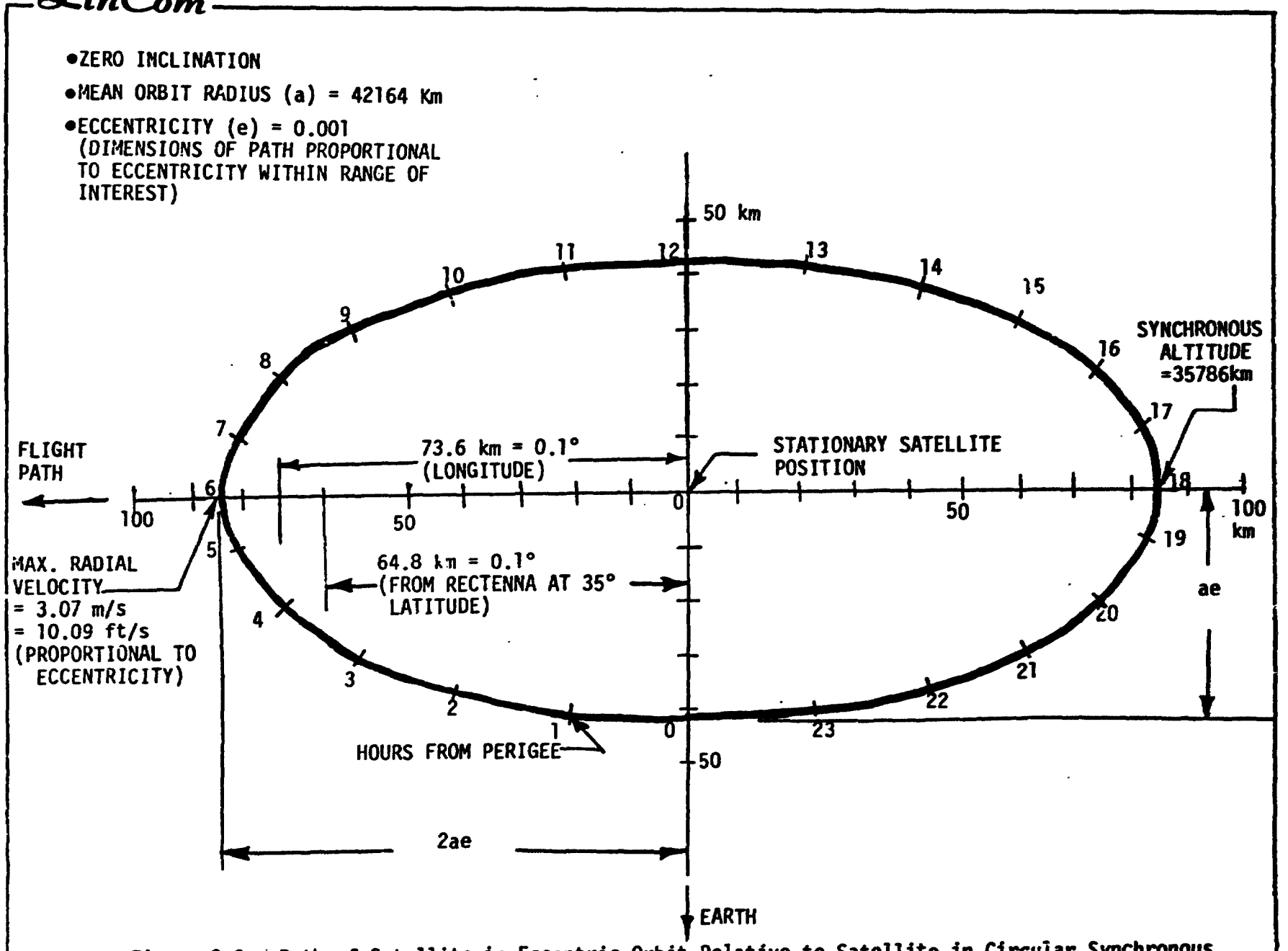

Figure 2.2. Path of Satellite in Eccentric Orbit Relative to Satellite in Circular Synchronous Orbit.

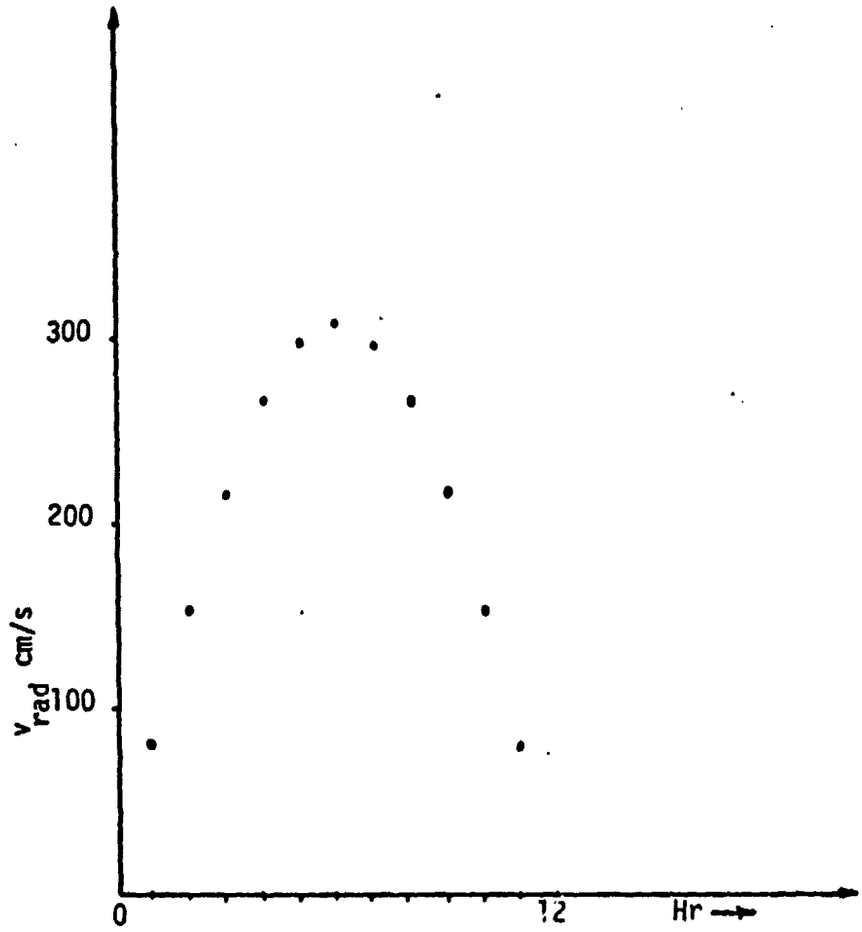

$$(\text{RADIAL ACCELERATION})_{max} = \frac{79.7 \text{ cm/s}}{1 \text{ hr.}}$$

$$= .02 \text{ cm/s}^2$$

Figure 2.3. Radial Velocity of SPS as a Function of Hour From Perigee.

geometry a little more carefully. In Fig. 2.4, we show the geometry of the SPS spacetenna with respect to the rectenna center on the ground. From this figure, we see that the radial velocity at each point on the spacetenna is different. The differential radial velocity of a point at a distance x from the center of a spacetenna is approximately

$$\Delta v = v_{rad} - v_{\beta}$$

$$\cong \frac{1}{2}\left[\frac{\cos\alpha}{R/x - \sin\alpha}\right]^2 v_{rad}$$

For our system, $R \cong 37{,}500$ Km, $x_{max} = 0.5$ Km. This gives

$$\frac{\Delta v_{max}}{v_{rad}} \cong \frac{1}{2}\left(\frac{1}{2x37{,}500}\right)^2 \cong 8.9 \times 10^{-11}$$

Since $v_{rad} \cong 300$ cm/s maximum, this corresponds to a maximum differential Doppler of 1.02×10^{-8} Hz . For all practical purposes, we can safely assume that all points on the spacetenna have identical radial velocity. The overall effect of the periodic motion of the satellite over 24 hrs is the addition of a common Doppler frequency to every signal transmitted to the rectenna center. However, they are still "inphase" as far as the coherency requirement at the rectenna center is concerned. In principle, there is no need to correct for this Doppler frequency variation; in practice, such a correction would assist the start-up procedure at the initial beam forming stage. We shall discuss methods to correct for the Doppler shift in a later section.

The above analysis only concludes that the problem associated with the elliptical orbit can be neglected when the satellite

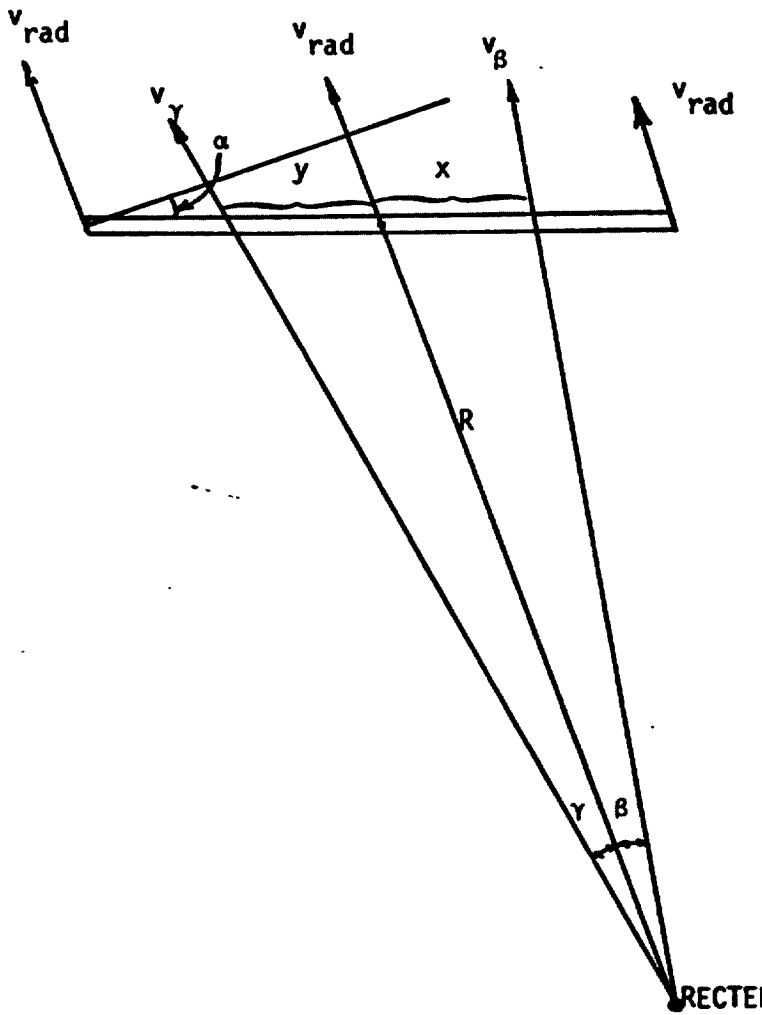

v_{rad} = radial velocity of the spacetenna structure

α = antenna tilt

$v_\alpha v_\gamma$ = radial component of point x and y

SUMMARY

$$v_\gamma = v_{rad} \cdot \cos \gamma$$

$$v_\beta = v_{rad} \cdot \cos \beta$$

$$\tan \gamma = \frac{\cos \alpha}{R/y + \sin \alpha}$$

$$\tan \beta = \frac{\cos \alpha}{R/x - \sin \alpha}$$

Figure 2.4. Geometry to Compute Radial Velocity on the Spacetenna.

tilt angle is held fixed. If, however, this angle rotates at a velocity $\dot{\alpha}$, an additional component of radial velocity is introduced, viz.,

$$v_\alpha = x\dot{\alpha}$$

where x is the distance from the center of the array. As an example, if $\alpha = 1$ $\widehat{\text{min}}$/sec, the differential velocity across the spacetenna is

$$v_\alpha = 1 \times \frac{2\pi}{60 \times 360} \times 10^3 \text{ m/sec}$$

$$= 0.29 \text{ m/sec}$$

which is approximately 2.4 wavelengths over 1 sec at 2.45 GHz. The resultant differential Doppler shift must be accounted for if the ground control concept is to be implementable. It is therefore important not only to specify the pointing accuracy α, but it is equally important to control the rate of change of α.

Random disturbances on the antenna due to the vibrations and structural bending that affect the nominal attitude and pointing of the spacetenna must also be accounted for. For these random processes, the autocorrelation functions are needed to assess the quantitative effect.

2.2 Ionospheric Effects

The random distribution of the electrons in the ionosphere and the depth of the ionosphere contribute to accumulation of phase errors in the beam wavefront. Ignoring for the moment the effects of the magnetic field of absorption at S-band, the total phase shift for a signal that travels from the spacetenna to the rectenna center is dependent on the frequency f and can be modeled by [3]

$$\phi(f) = \frac{2\pi L}{c} \cdot f - \frac{40}{f} \frac{2\pi}{c} \int N d\ell \qquad (2.2\text{-}1)$$

where

c = velocity of light in free space, 3×10^8 m/sec

L = path length from spacetenna to the rectenna center (37,500 Km)

$\int N d\ell$ = integrated electron density along the signal path

Equation (2.2-1) indicates that, at a fixed frequency, the phase shift is proportional to the path length and the number of electrons encountered along the signal path. A typical value for $\int N d\ell$ is $10^{17}/m^2$ column. It could vary by at least a factor of ten in each direction, i.e., from 10^{16} to $10^{18}/m^2$, depending upon the time of the day, the season, the position in the sunspot cycle and the geographical position [3]. Notice that irregularities in the ionosphere cause $\int N d\ell$ to change along different paths. If the ionosphere is turbulent (with moving irregularities), then $\int N d\ell$ can change as a random function of time along the same path. The rate of change of this quantity is of major concern to the successful design of a ground based phase control system.

2.2.1 Magnitude of the Phase Shift and 2π Ambiguity

Let us estimate the size of the phase shift given in (2.2-1). For $\int N d\ell = 10^{18}/m^2$ at f = 2.45 GHz,

$$\phi = \frac{2\pi}{3\times10^8} \times 37{,}500 \times 10^3 \times 2.45 \times 10^9 - \frac{40}{2.45\times10^9} \cdot \frac{2\pi}{3\times10^8} \times 10^{18}$$

$$= 1.92 \times 10^9 - 3.42 \times 10^2 \text{ rad}$$

In any phase measurement, one can only determine ϕ modulo 2π. Since ϕ is much greater than 2π, a direct measurement can only determine

its value up to multiples of 2π. This poses an obstacle in any average phase measurement scheme for a ground control purpose. For example, if we can measure $\langle\phi_1\rangle$ and $\langle\phi_2\rangle$ where the true phases are

$$\phi_1 = \langle\phi_1\rangle + 2k_1\pi$$

$$\phi_2 = \langle\phi_2\rangle + 2k_2\pi$$

Then

$$\frac{\langle\phi_1\rangle+\langle\phi_2\rangle}{2} = \frac{\phi_1+\phi_2}{2} - (k_1+k_2)\pi$$

Depending on whether (k_1+k_2) is odd or even, $\frac{\langle\phi_1\rangle+\langle\phi_2\rangle}{2}$ can be off by π from $(\phi_1+\phi_2)/2$ modulo 2π.

2.2.2 Group Delay and Filter Characteristics of the Ionosphere

If data is modulated onto a carrier at 2.45 GHz, the channel group delay is given by

$$\tau_g = \frac{d\phi}{d\omega} = \frac{L}{C} + \frac{1}{f^2}\frac{40}{C}\int N d\ell \qquad (2.2\text{-}2)$$

At $\int N d\ell = 10^{18}/m^2$, $\tau_g \cong 0.13 + 2.22\times10^{-8}$ sec. Aside from changing the group delay characteristic, the ionosphere also acts as a filter, whose differential (at Δf from $f = 2.45$ GHz) phase characterization is given by

$$\Delta\phi = \phi(f_0+\Delta f) - \phi(f_0)$$

$$= -\frac{2\pi}{f_0^2 C}\, 40 \int N d\ell \cdot \frac{\Delta f^2}{(f_0+\Delta f)} + \underset{\Delta f}{\text{linear term in}} \qquad (2.2\text{-}3)$$

This function is plotted in Fig. 2.5. From this figure, we see that the nonlinear phase shift introduced by the ionosphere is not too severe for $\Delta f \leq 100$ MHz.

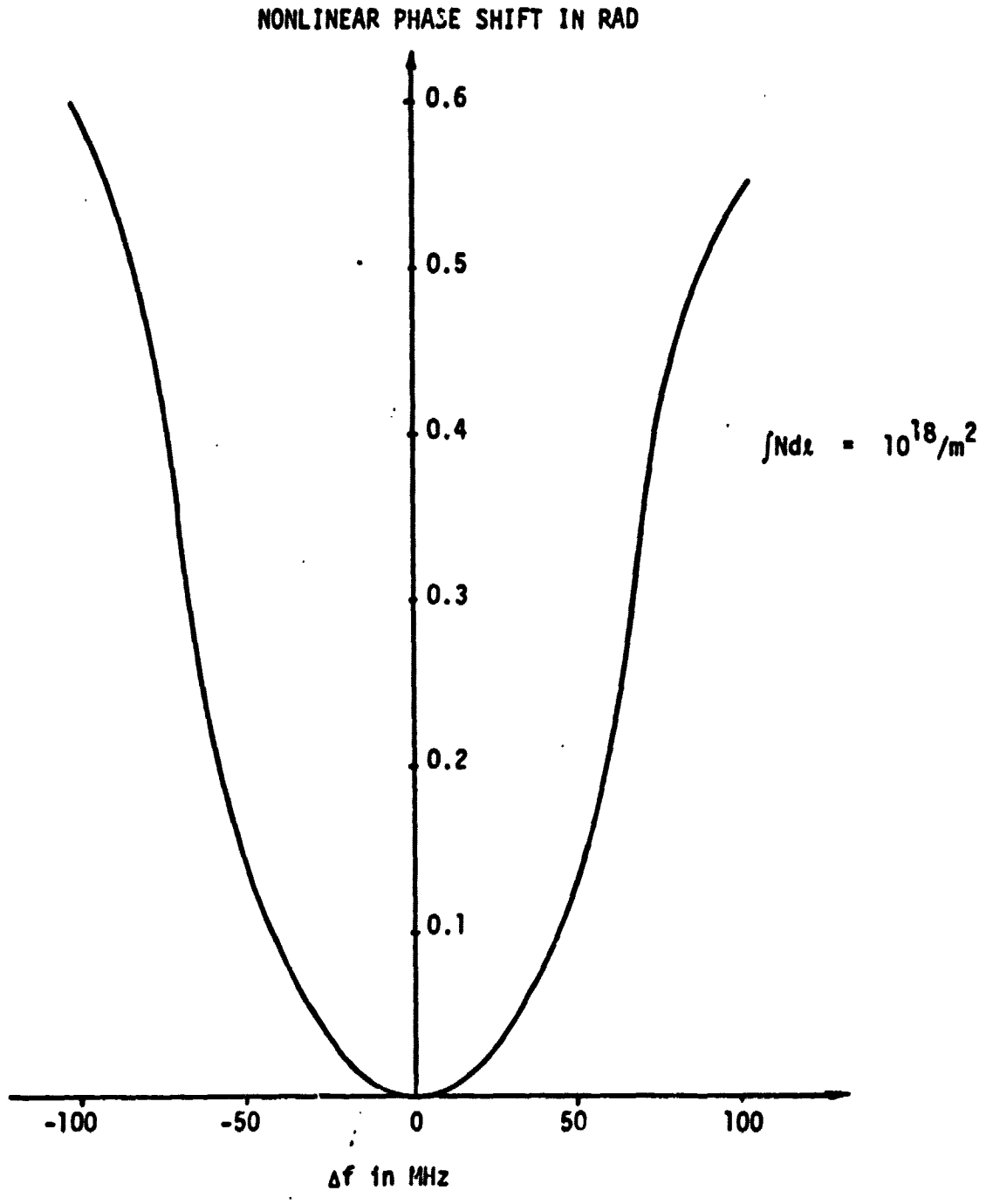

Figure 2.5. Nonlinear Phase Shift Exhibited by the Equivalent Characteristics Introduced by the Ionosphere.

2.3 Receiver Thermal Noise and Signal Power

The receiver noise power spectral density is given by the formula

$$N_0 = kt_0\overline{NF} \qquad (2.3\text{-}1)$$

where k is Boltzmann's constant (1.38×10^{-23} watt-sec/°K), t_0 = 290°K, and a typical value for the noise figure $\overline{NF}$ is 2.5 dB. For these values, N_0 = -201.5 dBW/Hz. It is of interest to size the received power on the ground due to one power beam (one power module). It is given by

$$P = \frac{P_T G_T A_R}{4\pi R^2} \qquad (2.3\text{-}2)$$

where

P_T = transmit power (65 KW)

A_R = Receive antenna area

$R = 3.8 \times 10^7$ m

$G_T = \eta\frac{4\pi A_T}{\lambda^2}$ = transmit antenna gain

η = transmit efficiency

A_T = transmit antenna area

λ = transmit wavelength at carrier frequency (0.12m)

For the SPS ground control concept, typical values for (2.3-2) are $A_R = \pi 5^2 m^2$ (10 m dish), η = 50%, and A_T varies from 1.155×2.6 m^2 to 5.2×5.2 m^2 depending on the location of the power module. In that case P varies from -64.3 dBW to -54.8 dBW. A typical value of the signal to noise spectral density level is then 136 dB-Hz minimum.

2.4 Interference from the Downlink Power Beam

For the input signal, a klystron amplifier has an equivalent filter characteristic depicted in Fig. 2.6. Outside the passband, the signal will be attenuated at a rate of 24 dB/octave or 80 dB/decade. The width of the passband determines the bandwidth of the measurement waveforms that can be used. In addition, a klystron amplifier generates phase noise of its own. Throughout this study, we shall adopt a measured model (Varian X-13) reflected to 2.45 GHz. The ratio of the single-sideband (SSB) power of the phase noise in a 1-Hz bandwidth f Hz away from the carrier, to the total signal power, is empirically given by ($f \geq 1$ kHz)

$$\mathcal{L}(f) = \frac{\alpha}{f^5} + \frac{\beta}{f^2} \quad \text{(in dBc/Hz)} \qquad (2.4\text{-}1)$$

where $\alpha = 1.58 \times 10^9$ and $\beta = 6.31 \times 10^{-4}$. $\mathcal{L}(f)$ is plotted in Fig. 2.7 for reference. The one-sided spectral density of the phase noise $S_\phi(f)$ is simply related to $\mathcal{L}(f)$ via

$$S_\phi(f) = 2\mathcal{L}(f) \qquad (2.4\text{-}2)$$

Let us proceed to compute the interference at the ground receiver caused by the phase noise characteristics of the klystrons. As an example, at f = 10 MHz, $\mathcal{L}(f)$ = -172 dBc/Hz = -124 dBW/Hz. Assuming a maximum transmit antenna area of $(5.2\text{m})^2$ and other parameters are the same as in Section 2.3, the space to ground link gives a loss of 103 dB. The phase noise level on the ground due to one klystron is therefore -124-103 = -227 dBW/Hz. Since there are 101,552 klystrons transmitting and the phase noise contribution adds up noncoherently, the resultant interference level is -227 + 50 + 3 = -174 dBW/Hz.

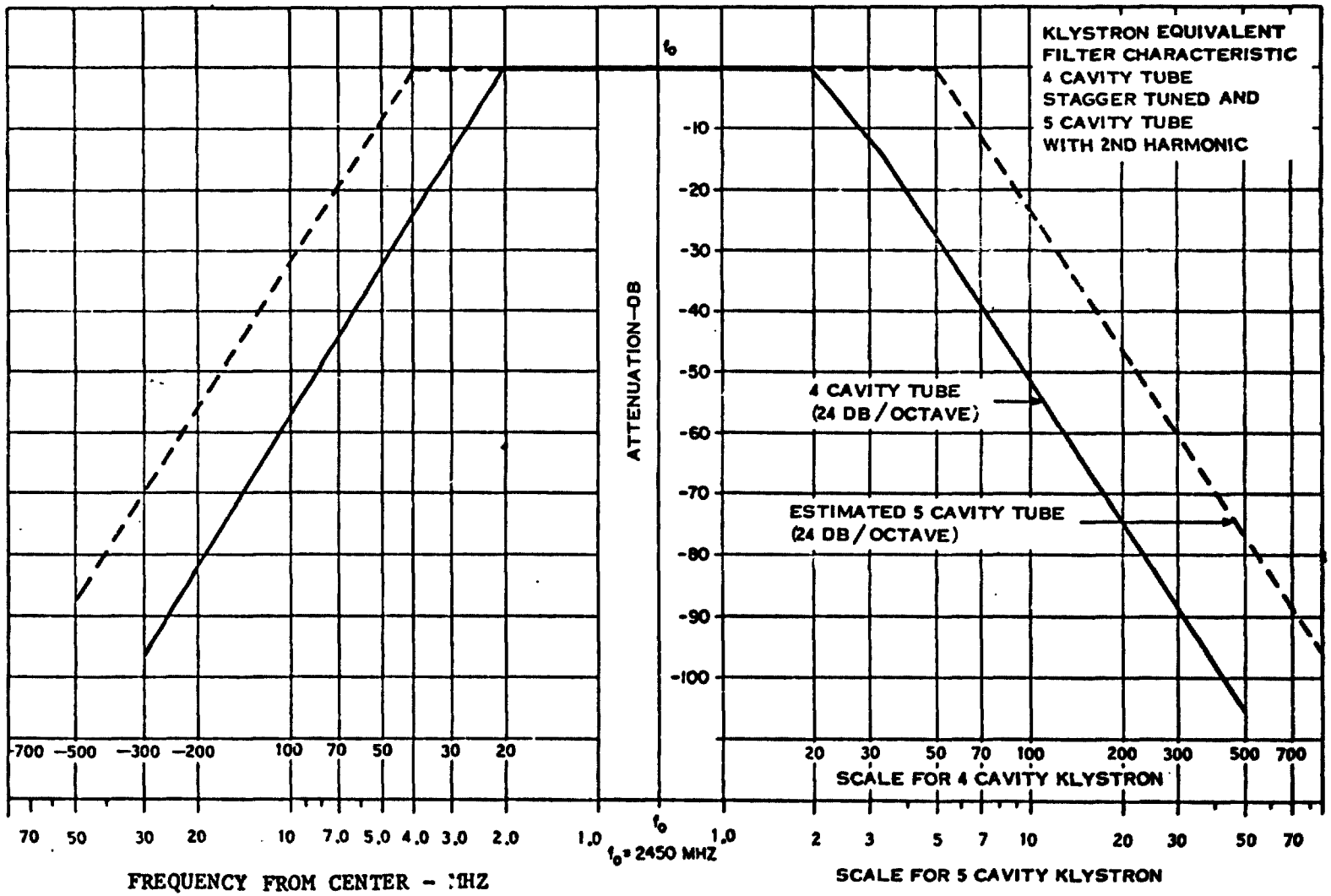

Figure 2.6. Klystron Equivalent Filter Characteristic.

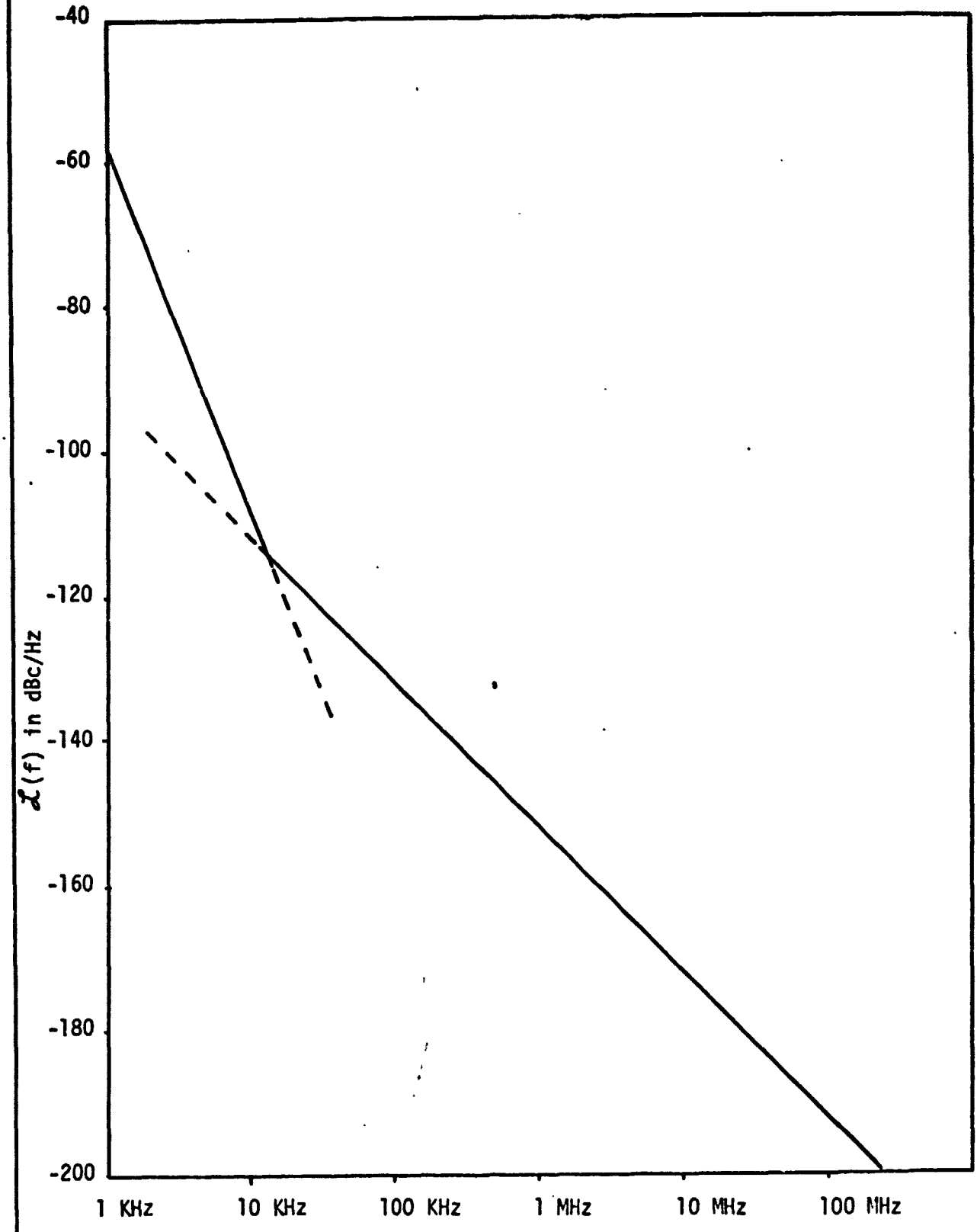

Figure 2.7. Klystron Phase Noise Model.

If we compare the phase noise contribution with the thermal noise contribution at -201.5 dBW/Hz, it is clear that the Klystron phase noise is the limiting component of intereference. The cross over point is roughly f = 100 MHz.

3.0 REQUIREMENTS FOR GROUND-BASED PHASE CONTROL SYSTEM

The ground-based phase control system configuration under study is given in Fig. 3.1. The key elements include:

(1) A Control Center (CC) on the satellite to schedule and distribute the phase error measurement waveform to the $i^{\underline{th}}$ power module (PM) at prescribed time slots (= 10 μs duration, cycled sequentially through 10^5 PMs), and to update the phase of the PMs.

(2) A communication system with capability to handle (covertly) uplink phase adjustment command, and to transmit a downlink pilot to establish a common phase and constant frequency reference for phase error measurements.

(3) A receiving antenna in the center of the rectenna for phase measurement, employed in a time-shared manner.

(4) A phase error measurement and filtering algorithm to determine the approximate phase correction for the individual PM.

In this particular configuration, the uplink and the downlink phase reference signals are considered to be physically separated from the spacetenna and rectenna. This configuration ensures the maximum isolation between the power beam and the communication signals. As a matter of fact, the uplink signal can be transmitted in a bent pipe mode via another satellite for added security protection and added anti-jamming capabilities. In that case, since the communication

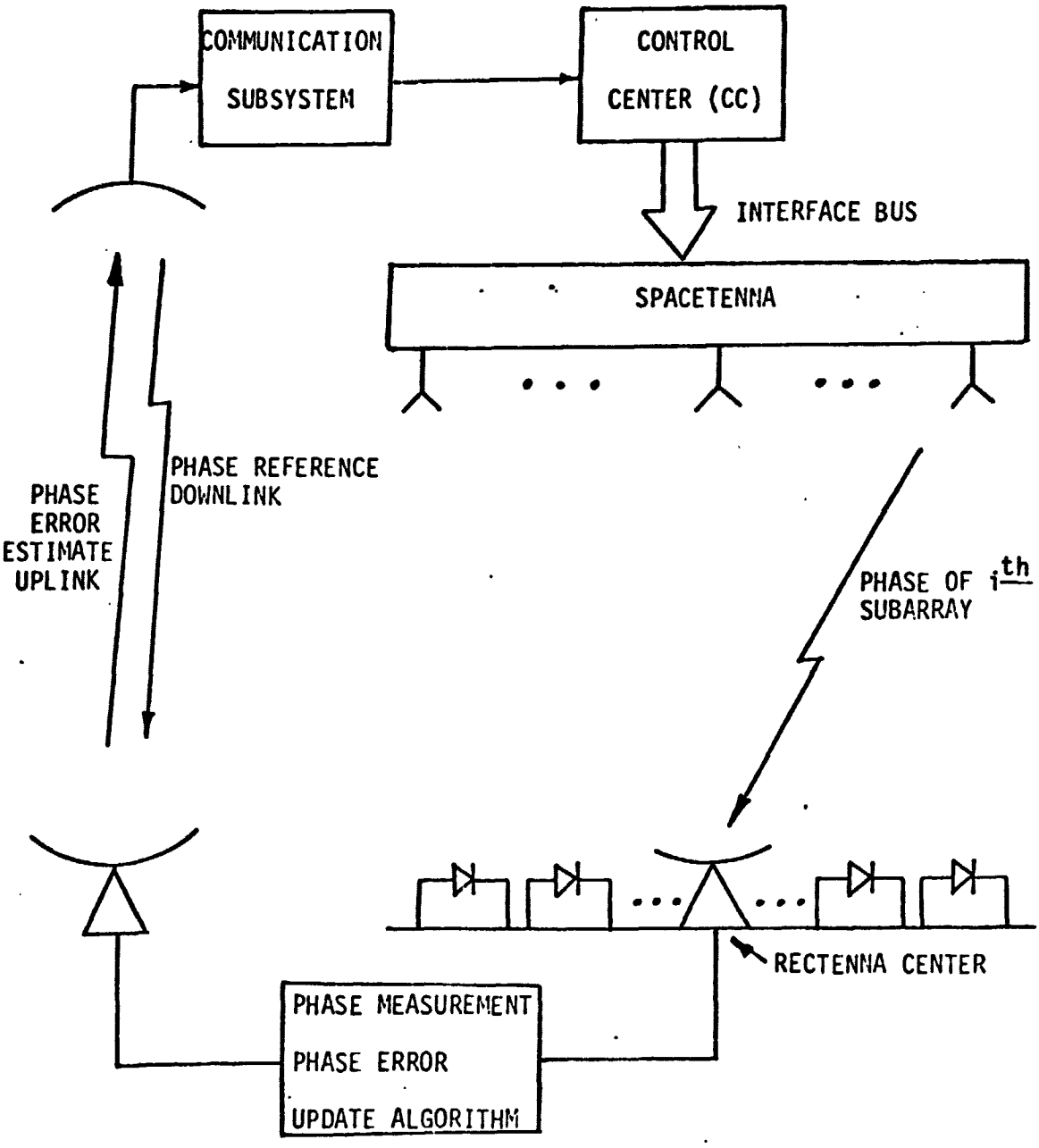

Figure 3.1. Ground Based Phase Control System Concept with Major Functional Blocks.

80 0056

antenna does not have to point in the direction of the power beam pattern, further signal isolation is possible.

The operation of the ground-based phase control system is described as follows. First of all a constant frequency reference is established on the ground using the downlink pilot signal. On the spacetenna, each PM will be switched to a measurement mode for 10 μsec in a predetermined sequential manner. The scheduling is provided by the control center on board SPS. During the measurement mode of the $i^{\underline{th}}$ PM, its arriving signal phase at the rectenna center is measured against the established reference. The measured phase error is used as an input to the $i^{\underline{th}}$ phase error update algorithm. The resultant phase error estimate is sent to SPS via the uplink signal path. The communication subsystem demodulates the uplink data and the phase error updates are processed by the control center. The phase corrections are then routed to the appropriate PM via the interface bus. Of course, the successful operation of the system hinges on the synchronized time division operations described above. In what follows, we describe in detail various possible schemes to implement the subsystem functions described earlier. Their merits are judged by their performance under the set of channel constraints discussed earlier. In this section, we assume that the ionosphere is nonturbulent in nature, i.e., $\int N d\ell$ along a particular path in (2.2-1) cannot change significantly in a time frame of roughly 10 secs.

3.1 Downlink Reference Pilot Waveform Design

A reference on the ground at the same frequency of the downlink power beam is needed to line up the individual power beams. In this capacity, there is no phase coherency requirement between the SPS and the ground

reference since the individual power beams is to be lined up after the ground reference is established. When this fact is taken into consideration, we can use a pilot signal at two times the power beam frequency (2 x 2.456 Hz = 4.90 GHz), which must be derived from the common frequency standard used on board the SPS. (In essence, we want all frequencies to be derived from the same source so as to nullify the effect of frequency drifts.) This signal is then tracked on the ground and divided down to 2.45 GHz to be used as the frequency reference. The bandwidth of the tracking loop should be wide enough to track out the Doppler induced by the satellite motion (300 cm/s maximum). For our system, the maximum Doppler frequency is approximately 50 Hz/sec at 4.9 GHz. Notice that after the divide by two circuit, the Doppler shift due to the satellite motion will be the same as the individual power beams. The advantage of this scheme is that it provides a frequency separation between the power beam and the reference. This can substantially simplify the downlink pilot reference receiver design. The pilot signal should be PN spread for security.

Other approaches are also possible. For example, one can use the formed power beam as a common reference for phase measurement. The main disadvantage with this approach is that some kind of acquisition aid must be used before the beam is formed. One would also expect the time required to form the beam in the initialization stage is longer than the first scheme. An alternative approach is to send a reference downlink from which a phantom frequency of 2.45 GHz can be reconstructed, e.g., using a two tone scheme.

3.2 Phase Error Measurement Waveforms and Techniques

In the current concept, each PM will be transmitting in the phase measurement mode for 10 μsec. Since we have to accomplish the phase comparison in a relative short time interval, we prefer the measurement waveform format to be as simple as possible. The 10 μsec constraint also restricts the bandwidth of the input IF filter for interference suppression. The minimum bandwidth that can be employed is approximately 1 MHz to guarantee a sufficiently fast rise time. There are two distinct types of waveform formats to choose from, namely, a data (PN) modulated suppressed carrier or unmodulated sidetones. If we use unmodulated tones with a phantom carrier, there is a need to resolve the π ambiguity introduced in recreating the carrier at 2.45 GHz as described in Section 2.2. The advantage with this scheme is its simplicity and the high signal to interference ratio attainable as we can get by with a narrow bandwidth IF filter. On the other hand, if we PN modulate the carrier, the problem with the phase ambiguity is absent since the ionosphere then acts as a channel filter with nonlinear phase shift. The nonlinear phase shift only tends to increase data distortions and is discussed in Section 2.2. However, a wider IF filter bandwidth is required. This will degrade the signal-to-interference ratio.

In order for a measurement scheme to function properly, we also require that the PMs switch to the measurement mode at the precise allocated time slot. Otherwise, any overlap signals will interfere with one another. If PN-modulated data is used, the chip rate should be as low as possible so that temporal path delay variations cannot affect the arrival time of the data from the control center to the PM locations, to within 10% of a chip time.

3.2.1 Two-Tone Phase Measurement Scheme with Coherent Subcarrier

In the basic two-tone measurement scheme, two side tones at $f_0 \pm \Delta f$ are transmitted from the satellite to the ground receiver. A phantom carrier can be reconstructed from the sidetones by passing the signal through a squaring circuit. The output will then have a CW component with frequency $2f_0$ and a phase component equal to $(\phi_1+\phi_2)$, where ϕ_1 and ϕ_2 are the channel induced phase shifts at $f_0+\Delta f$ and $f_0-\Delta f$, respectively. This phase shift is very close to double the one that would have occurred if the downlink signal were a single sinusoid at frequency f_0. Their differences can be determined by eq. (2.2-1) in Section 2.2. If we divide the $2f_0$ component by two, we obtain the average phase $\frac{\phi_1+\phi_2}{2}$. Unfortunately, the divide by two circuit results in a 0°-180° ambiguity.

We shall now consider a modified two-tone scheme that is relatively simple in concept. The idea is to use the coherency of the subcarrier for ambiguity resolution. This scheme is given in Fig. 3.2. When the $i^{\underline{th}}$ PM is switched to the measurement mode, the waveform at the input to the HPA is (ignoring multiplicative constants)

$$s_1(t) = \cos[(\omega_0 t+\theta_i)\frac{2M+1}{2M} + \frac{\pi k}{M}] + \cos[(\omega_0 t+\theta_i)\frac{2M-1}{2M} - \frac{k\pi}{M}]$$

where θ_i includes the commandable phase shift and $\frac{k\pi}{M}$ results from the ambiguity introduced by the divide by 2M circuit. At the receiver on the ground,

$$s_2(t) = \cos[(\omega_0 t+\theta_i)\frac{2M+1}{2M} + \frac{k\pi}{M} + \gamma_1] + \cos[(\omega_0 t+\theta_i)\frac{2M-1}{2M} - \frac{k\pi}{M} + \gamma_2]$$

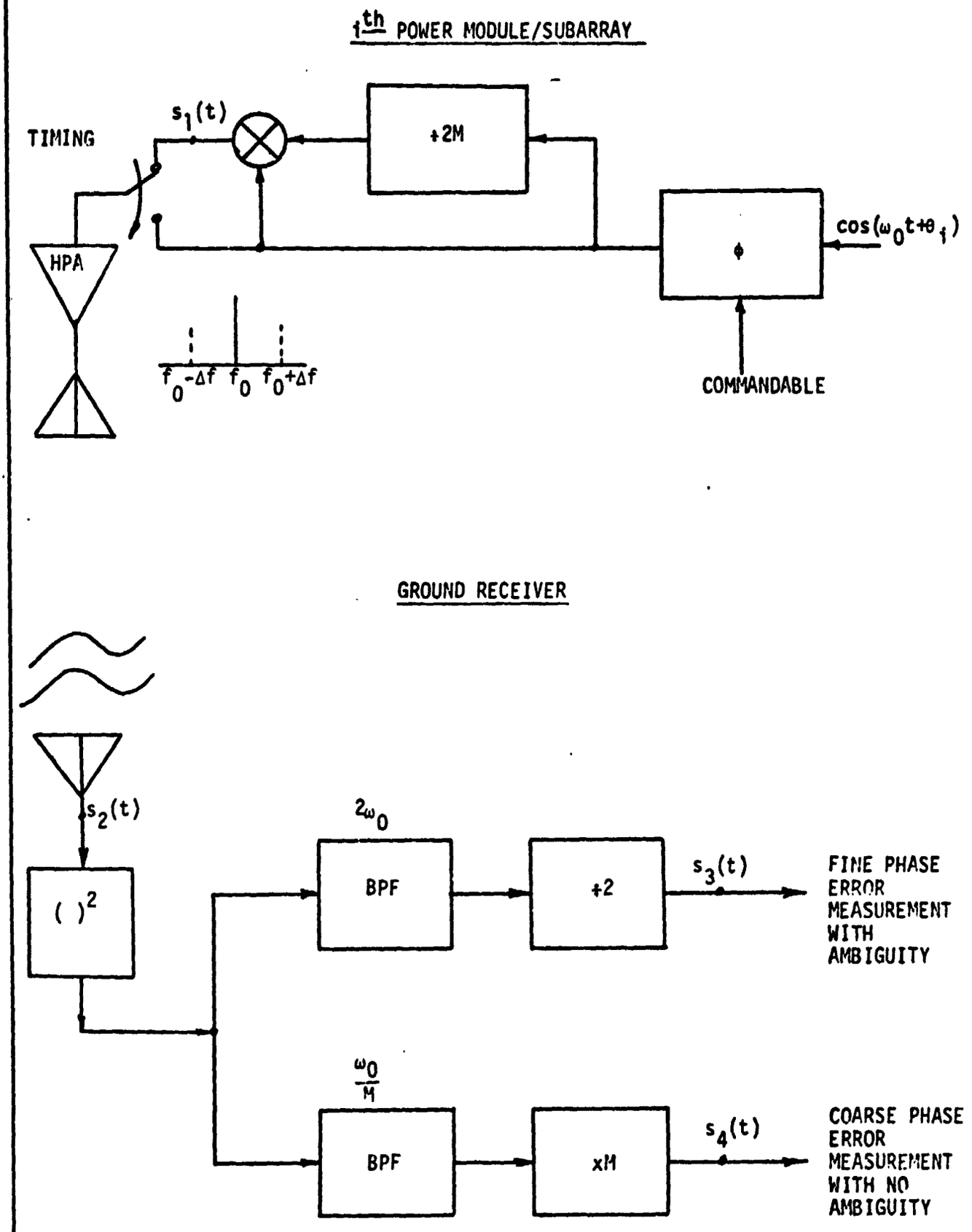

Figure 3.2. Two Tone Measurement Technique with Coherent Subcarrier for Ambiguity Resolution.

where the tones are offset from the phantom carrier by $\Delta f = \pm\frac{f_0}{2M}$ and φ_1 and φ_2 are the frequency dependent phase shifts introduced by the downlink path and the ionosphere. It is then easy to check that the signals $s_3(t)$ and $s_4(t)$ are given by

$$s_3(t) = \pm\cos[\omega_0 t + \theta_1 + \frac{\varphi_1+\varphi_2}{2}]$$

and

$$s_4(t) = \cos[\omega_0 t + \theta_1 + M(\varphi_1-\varphi_2)]$$

Notice that $s_3(t)$ is the desired phantom carrier except for the sign ambiguity. This ambiguity can be resolved using $s_4(t)$ since $M(\varphi_1-\varphi_2)$ is approximately constant for all 101,552 paths. One only needs to slip the sign of $s_3(t)$ selectively so that its phase relationship with $s_4(t)$ is the same for all 10^5 different measurement signals.

Up to now we have neglected the effect of interference . If this is included, we see that $s_4(t)$ is a relatively noisy signal because the phase noise introduced by the channel interference is multiplied by M. For example, we have M = 100 for Δf = 12.25 MHz. The noise power at the output of $s_4(t)$ will be roughly 10^4 times the noise power for $s_3(t)$. Improvements of this basic scheme to reduce M is possible. The idea is to modulate the subcarriers at $f_0 \pm \Delta f$ with coherent data or tones and use them for ambiguity resolution. The details will not be pursued here.

3.2.2 Four-Tone Phase Measurement Scheme

The four-tone measurement scheme given in Fig. 3.3 is a simple modification of the two-tone scheme. Basically, we first use frequencies at $f_0 \pm 2\Delta f$ for phase error measurement which introduces π ambiguity. Then we use frequencies at $f_0 \pm \Delta f$ for ambiguity resolution. The scheme works as follows. The transmitted signal at the input to the transmitting antenna is (neglecting multiplicative constants)

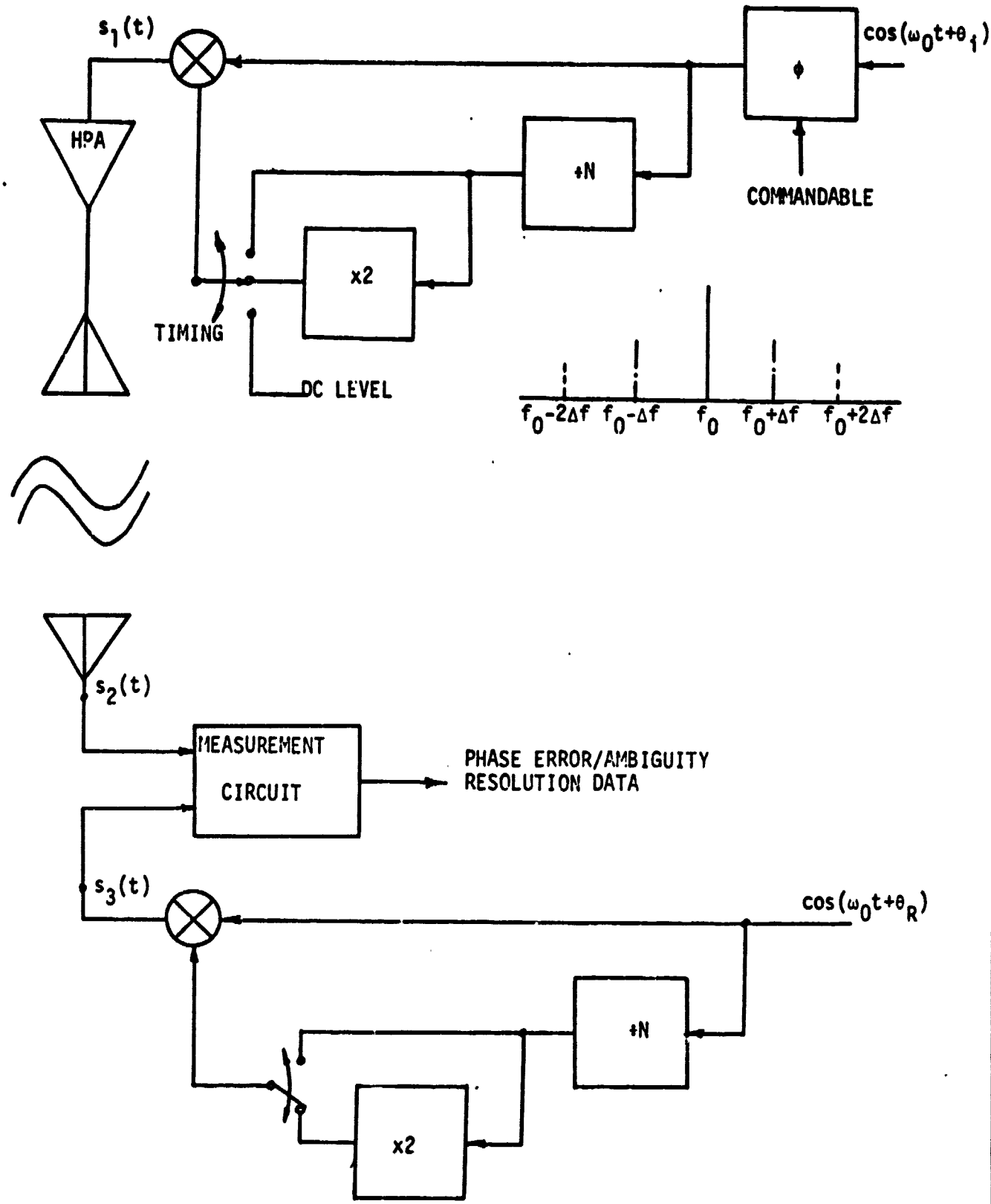

Figure 3.3 Four-Tone Phase Measurement Scheme.

$$s_1(t) = \cos[\omega_0(1+\tfrac{\ell}{N})t + (1+\tfrac{\ell}{N})\theta_1 + \tfrac{2\pi k\ell}{N}]$$

$$+ \cos[\omega_0(1-\tfrac{\ell}{N})t + (1-\tfrac{\ell}{N})\theta_1 - \tfrac{2\pi k\ell}{N}] \quad \ell = 0,1,2$$

where θ_1 includes the commandable phase shift, $\frac{2k\pi}{N}$ is the ambiguity introduced by the divide by N circuit, $\Delta f = \frac{f_0}{N}$, and $\ell = 0,1,2$ depending on whether the PM is in the power mode (1), ambiguity resolution mode (2), or phase error measurement mode (3). At the receiver on the ground,

$$s_2(t) = \cos[\omega_0(1+\tfrac{\ell}{N})t + (1+\tfrac{\ell}{N})\theta_1 + \tfrac{2\pi k\ell}{N} + \varphi_+(\ell)]$$

$$+ \cos[\omega_0(1-\tfrac{\ell}{N})t + (1-\tfrac{\ell}{N})\theta_1 - \tfrac{2\pi k\ell}{N} + \varphi_-(\ell)]$$

where $\varphi_+(\ell)$ and $\varphi_-(\ell)$ are the phase shifts introduced by the channel. The reference signal $s_3(t)$ is given by

$$s_3(t) = \cos[\omega_0(1+\tfrac{\ell}{N})t + (1+\tfrac{\ell}{N})\theta_R + \tfrac{2\pi\ell m}{N}]$$

$$+ \cos[\omega_0(1-\tfrac{\ell}{N})t + (1-\tfrac{\ell}{N})\theta_R - \tfrac{2\pi\ell m}{N}]$$

where θ_R is the phase of the ground reference, and $\frac{2\pi m}{N}$ is the ambiguity introduced by the ground divide by N circuit. If the operations are synchronized, we can then measure up to modulo 2π at the output of the measurement circuit, the phases

$$\varphi_+(\ell) + (1+\tfrac{\ell}{N})(\theta_1-\theta_R) + \tfrac{2\pi\ell}{N}(k-m) = \phi_+(\ell) + 2\pi M_+(\ell) \qquad (3.2\text{-}1)$$

$$\varphi_-(\ell) + (1-\tfrac{\ell}{N})(\theta_1-\theta_R) - \tfrac{2\pi\ell}{N}(k-m) = \phi_-(\ell) + 2\pi M_-(\ell) \qquad (3.2\text{-}2)$$

Actually, in (3.2-1) and (3.2-2), $\phi_+(\ell)$ and $\phi_-(\ell)$ are the measured phases and $M_+(\ell)$ and $M_-(\ell)$ are integers so that the absolute values

of $\phi_+(\ell)$ and $\phi_-(\ell)$ can be restricted to π. Note that we are interested in determining $[\phi_+(\ell)+\phi_-(\ell)]/2$ modulo 2π. For $\ell=2$, we know from (3.2-1) and (3.2-2) that

$$\frac{\phi_+(2)+\phi_-(2)}{2} = \frac{\phi_+(2)+\phi_-(2)}{2} + [M_+(2)+M_-(2)]\pi-(\theta_1-\theta_R) \quad (3.2\text{-}3)$$

Now if we can resolve whether $[M_+(2)+M_-(2)]$ is even or odd, we can determine $[\phi_+(2)+\phi_-(2)]/2+(\theta_1-\theta_R) \bmod 2\pi$. This information is provided by comparing

$$\phi_+(1) - \phi_-(1) = -\frac{2}{N}(\theta_1-\theta_R) - \frac{4\pi}{N}(k-n) + \phi_+(1) - \phi_-(1) + [M_+(1)-M_-(1)]2\pi \quad (3.2\text{-}4)$$

$$\frac{\phi_+(2)-\phi_-(2)}{2} = -\frac{2}{N}(\theta_1-\theta_R) - \frac{4\pi}{N}(k-n) + \frac{\phi_+(2)-\phi_-(2)}{2} + [M_+(2)-M_-(2)]\pi \quad (3.2\text{-}5)$$

If Δf is designed properly ($\Delta f < 50$ MHz) the left hand side of (3.2-4) and (3.2-5) are nearly equal. (See Section 2.2 for the discussion on ionospheric effects.) Equating (3.2-4) and (3.2-5) we have

$$\frac{\phi_+(2)-\phi_-(2)}{2} + [M_+(2)-M_-(2)]\,\pi \equiv \phi_+(1) - \phi_-(1) \pmod{2\pi} \quad (3.2\text{-}6)$$

Since we can measure $\phi_+(\ell)$, we can determine from (3.2-6) whether $[M_+(2)-M_-(2)]$ is odd or even. This then determines whether $[M_+(2)+M_-(2)]$ is odd or even, since $[M_+(2)-M_-(2)] + [M_+(2)+M_-(2)] = 2M_+(2)$ must be even. With this information, we can solve for $[\phi_+(2)+\phi_-(2)]/2 + (\theta_1-\theta_R)$ modulo 2π in (3.2-3).

3.2.3 Data Modulation Schemes

A representative data modulation phase error measurement scheme is given in Fig. 3.4. A PN sequence with a bi-ϕ modulation format is used to spread the carrier. At the receiver on the ground, the

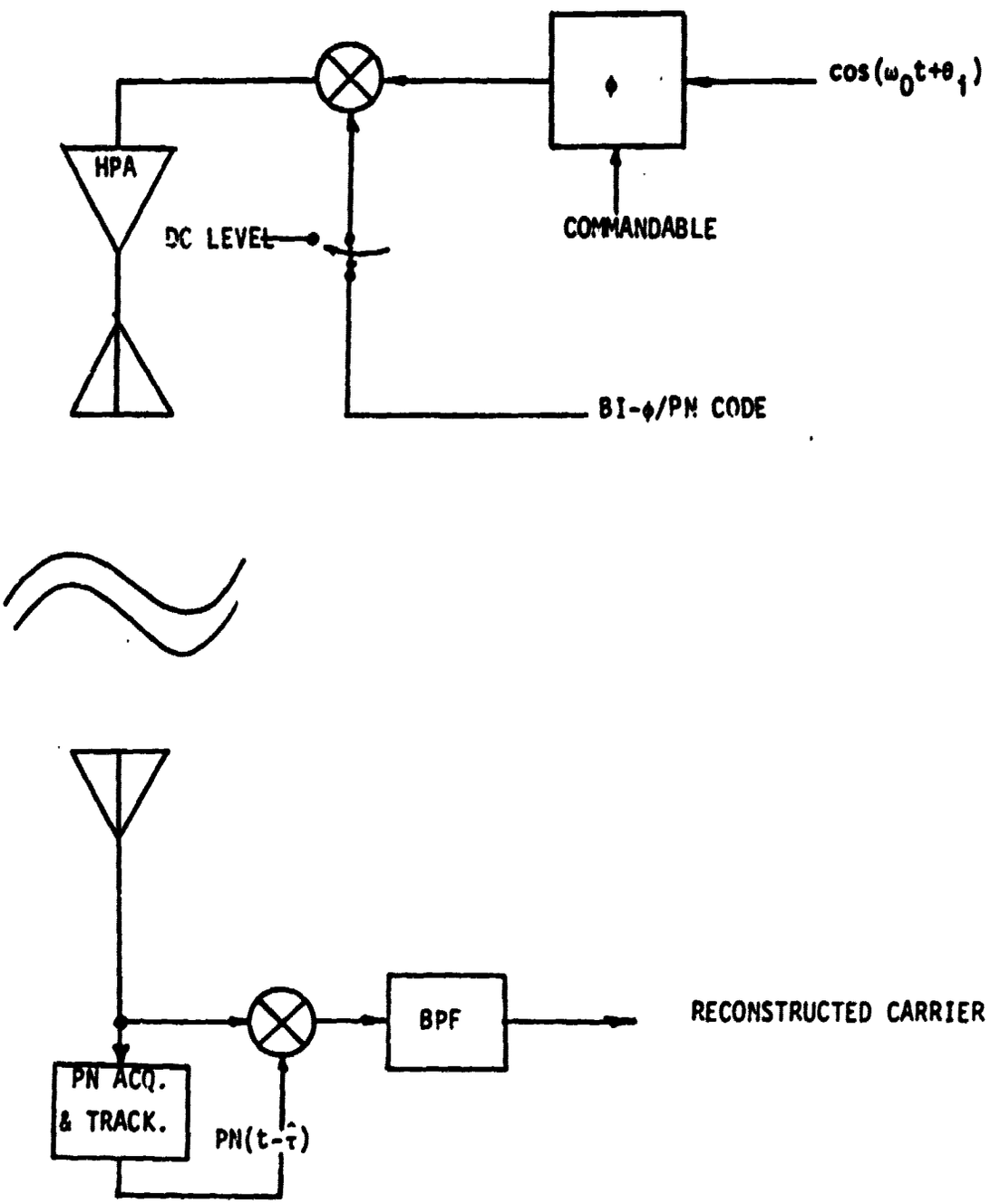

Figure 3.4. Data Modulation Phase Error Measurement Schemes.

signal is despread to obtain the carrier. The PN tracking is done via a noncoherent delay lock loop. (Until the beam is formed, the arriving phases from different PMs are not the same.) This scheme requires that the PN signal arriving at each PM switches at the same time. Otherwise, the despreader on the ground cannot function properly. One advantage of this approach is that timing can be derived directly from the received PN signal. For we can identify each PM with a particular state in the PN generator. However, a wide enough IF bandwidth to pass the PN signal is required on the ground receiver. The resulted higher interference level may prove troublesome.

3.3 Phase Error Measurement

In this section, we present a model to compute the signal-to-noise ratio of the phase error estimates. This model is illustrated in Fig. 3.5. The reconstructed carrier is filtered and then mixed down to baseband using the I and Q components of the ground frequency reference. Since the reconstructed carrier and the reference has the same Doppler shift, the outputs of the mixers are proportional to $\cos(\theta_i-\theta_R)$ and $\sin(\theta_i-\theta_R)$ where θ_i is the incoming phase of the signal from the $i^{\underline{th}}$ PM and θ_R is the phase of the reference. They are then integrated over T = 10 μsec to improve the signal to noise ratio and the results are used to determine $\theta_i-\theta_R$, e.g., by computing $(\theta_i-\theta_R) = \tan^{-1}[\sin(\theta_i-\theta_R)/\cos(\theta_i-\theta_R)]$. (The raw data can also be used directly in the phase update algorithm.) For a numerical example, we consider the four-tone measurement method with the two tones for phase measurement be offset 10 MHz from the center frequency. The signal to interference PSD level before carrier reconstruction is roughly -64 + 174 = 110 dB/Hz. (See discussions in Section 2.) Assuming a 3 dB loss in signal power

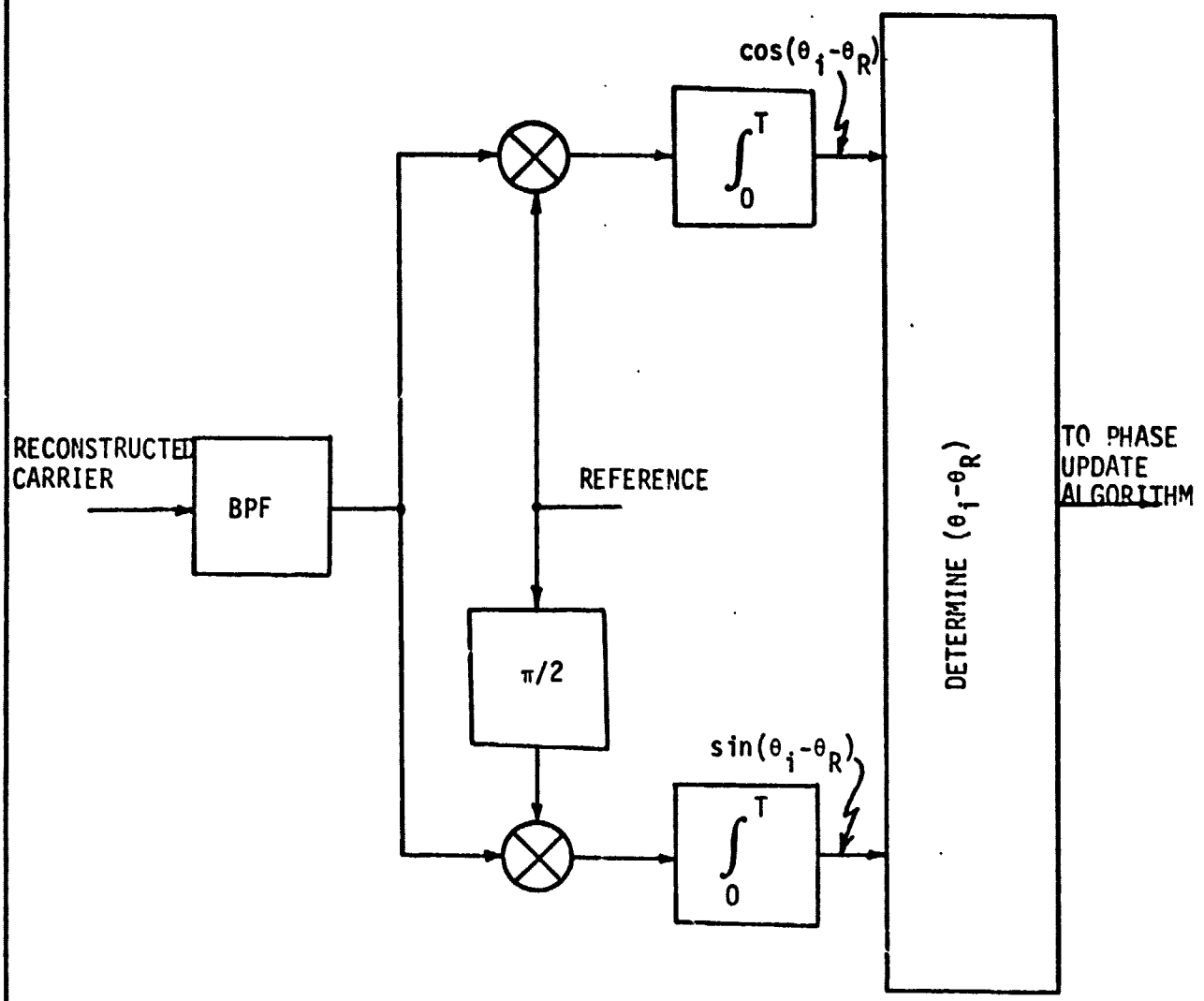

Figure 3.5. Model for Phase Error Measurement.

for the carrier reconstruction, we have at the output of the integrate and dump a signal to noise ratio of roughly 107-50 = 57 dB. This signal to noise ratio should give us a very comfortable margin.

3.4 Phase Error Updating Algorithm

The calibration of the transmitted phase at the PM is handled by a phase update algorithm stored in a computer for each individual PM. A functional block diagram of the scheme is depicted in Fig. 3.6. In Fig. 3.6, we show the phase error for each individual PM is processed separately by the ground computer. The filtered phase corrections are then formatted into a serial fashion and sent to the SPS via the uplink path.

A simplified model of the phase update algorithm for the ground control scheme is shown in Fig. 3.7. In the figure n_k is the equivalent phase noise generated by the channel, ψ represents the deterministic offset due to satellite motion, mean ionospheric trend, bias, etc., z^{-1} denotes the delay operator, and $D(z^{-1})$ represents a digital filter. Our purpose is to adjust the transmitted phase at the PM so that the arriving signal phase at the ground receiver is lined up with the ground reference. The operation is described by the stochastic difference operator equation

$$\phi_k = \theta_R - [n_k + \psi_0 + \theta_0 - \frac{z^{-1}D(z)}{1-z^{-1}} \phi_k]$$

Or, simply,

$$[1-z^{-1}+z^{-1}D(z)]\phi_k = (1-z^{-1})(\theta_R-\theta_0-\psi-n_k) \qquad (3.4\text{-}1)$$

As an example, if $D(z) = \alpha$ for $1-|\alpha| < 1$, (3.4-1) reduces to

$$\phi_k = (1-\alpha)\phi_{k-1} - (n_k-n_{k-1}) - (\psi_k-\psi_{k-1}) \qquad (3.4\text{-}2)$$

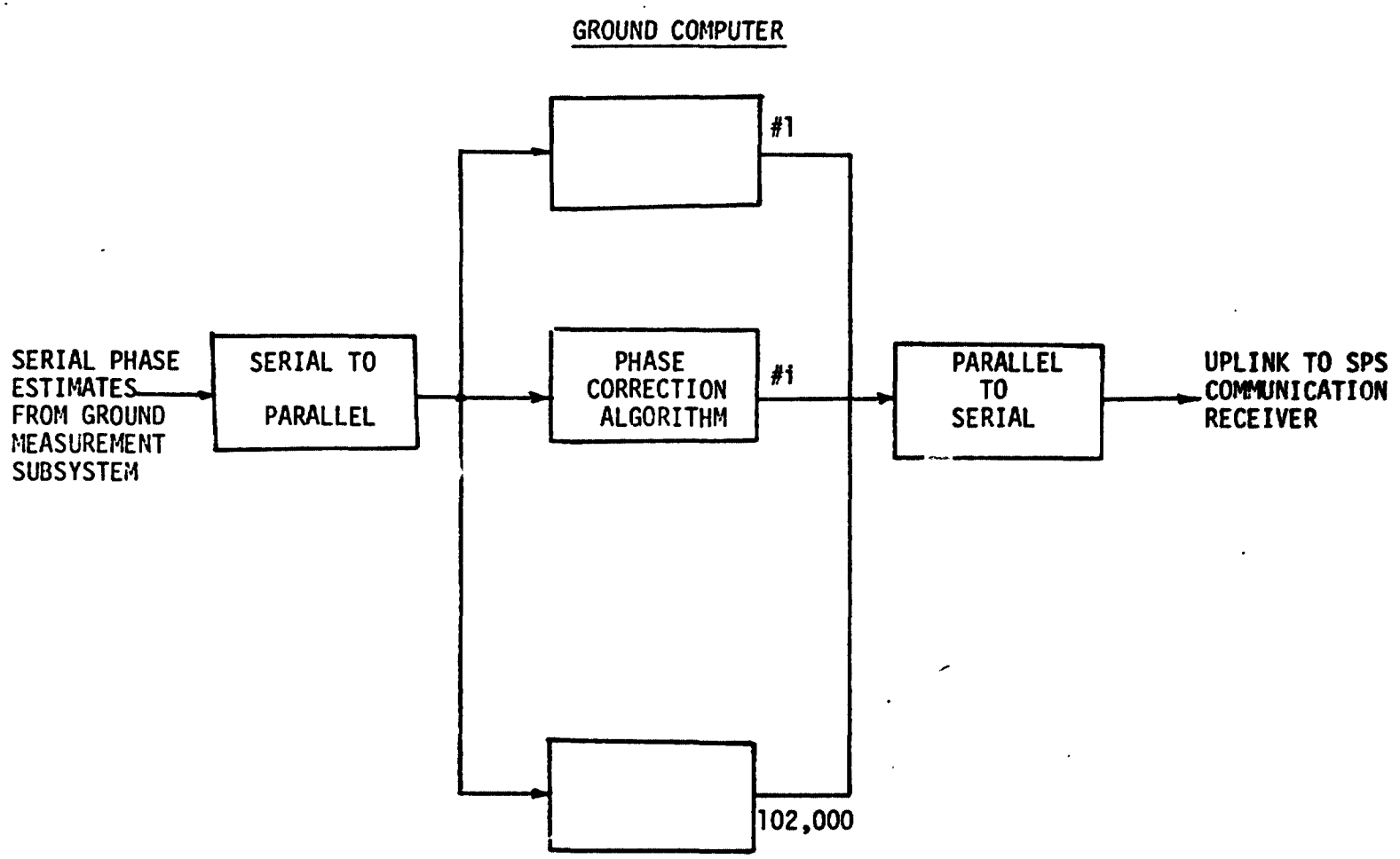

Figure 3.6. Ground Based Phase Iteration Scheme.

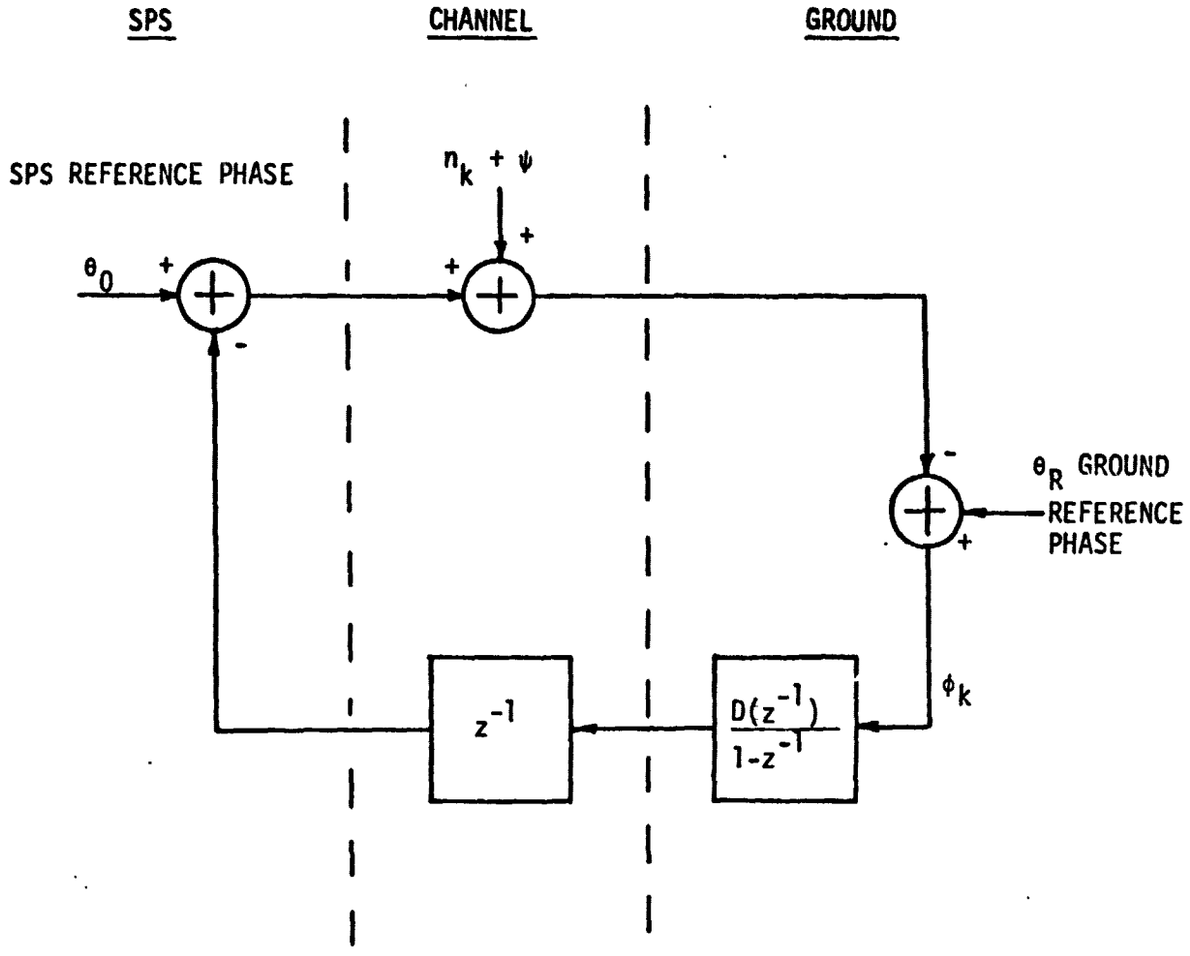

Figure 3.7. Equivalent Mathematical Model for Phase Update Algorithm.

It is readily shown that $\{\phi_k\}$ will approach to a steady state limit ϕ_s with zero mean as $k \to \infty$.

In general, the choice of the filter D(z) will be determined by the channel conditions discussed in Section 2.2.

3.5 Uplink Phase Correction Command Format

The phase updates for the PMs will be transmitted to the SPS communication receiver employing PN/QPSK modulation via a convenient carrier other than 2.45 GHz to avoid interference from the power beam. The uplink command format is given in Fig. 3.8. The data rate is approximately 1.02×10^5 bit/sec. The choice of the chip rate depends on the desired processing gain and the security requirement on the uplink commands. The uplink signal can be divided into identical frames with a period of approximately 1 sec. Within each frame, the data is divided into 1+101,552 slots. The first slot is the header and is devoted to synchronization and station identification purpose. The rest of the frame is divided into 101,552 slots of 10 bit data. The data in the $i^{\underline{th}}$ slot represents the quantized phase correction for the $i^{\underline{th}}$ power module. The end of the header signals the first PM correction and the rest follows sequentially. The numbering scheme of the PM is assumed to be known. For added security, the slot position can be scrambled on the ground and the key for unscrambling is passed along in the ID code. The function of the satellite control center is to process the uplink command and relay the phase corrections to the appropriate PMs, along with other pertinent informations.

3.6 System Synchronization

The main purpose of the SPS synchronization system is twofold:

(1) On the satellite, to switch on and off the calibration mode

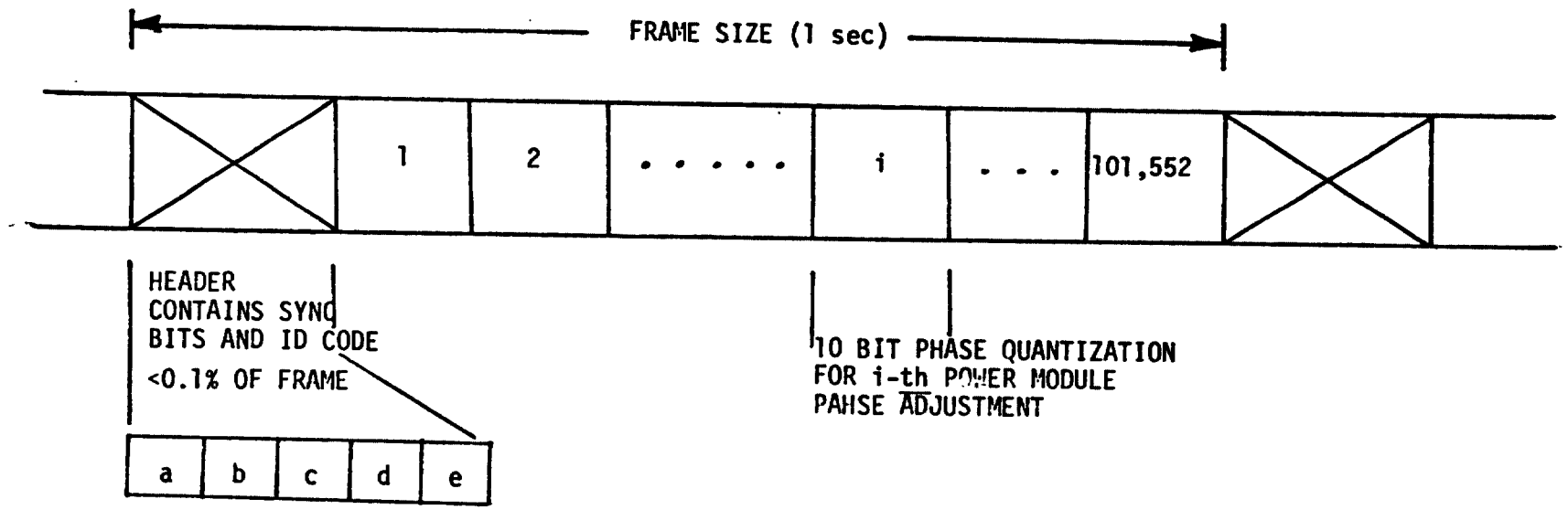

(a) GUARD TIME

(b) UNIQUE WORD

(c) STATION ID CODE

(d) COMMAND AND CONTROL DATA

(e) OTHERS

DATA RATE REQUIREMENT = 1.02×10^6 bit/sec

Figure 3.8. Uplink Command Format.

for each PM at the allocated time slots, so that the measurement signals for different PMs will not overlap and interfer with one another.

(2) On the ground receiver, to recognize the time slots devoted to different PMs.

Depending on the measurement scheme adopted, we have identified two representative approaches.

3.6.1 Data Modulated Carrier

If PN modulated carrier is used for calibration measurement, the system synchronization function is almost built-in. All we have to do is to pick a particular state of the PN generater (e.g. all 1's) to be the starting point for calibration #1 (#1PM). The sync waveform on the SPS required is depicted in Fig. 3.9.

3.6.2 Four-Tone Measurement Scheme

The synchronization scheme with four-tone calibration measurement is a bit more elaborate. The sync waveform for the PM's is depicted in Fig. 3,10. The start of the calibration cycle is denoted by an interval in which all PMs are in the power mode. This interval can easily be detected on the ground by a power measurement at the appropriate channel ($\pm\Delta f$, $\pm 2\Delta f$) output. The phase correction procedure (at $\pm 2\Delta f$) is first used until the arriving phases for individual beams are multiples of π within one another. This state can easily be detected either on the ground or on the SPS by examining the size of the correction steps. Then the measurement waveforms are switched to the ambiguity resolution mode (at Δf). After the ambiguity is resolved, the SPS waveforms will be switched back to the measurement mode and stay there. Periodically, we can recalibrate the π ambiguity by switching to the ambiguity resolution mode.

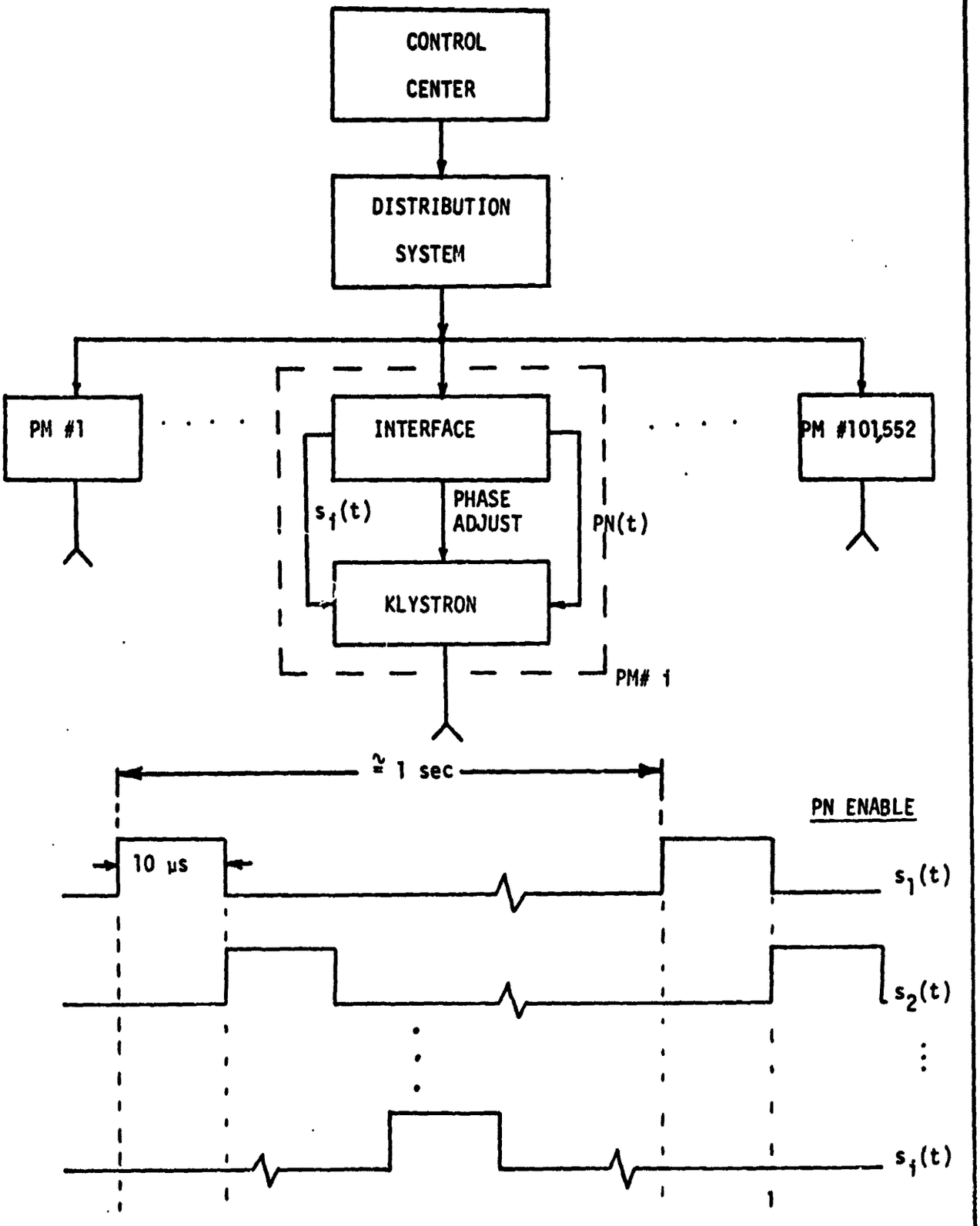

Figure 3.9. Sync Waveform on the Satellite for Bi-ϕ Modulated Carrier Measurement Scheme.

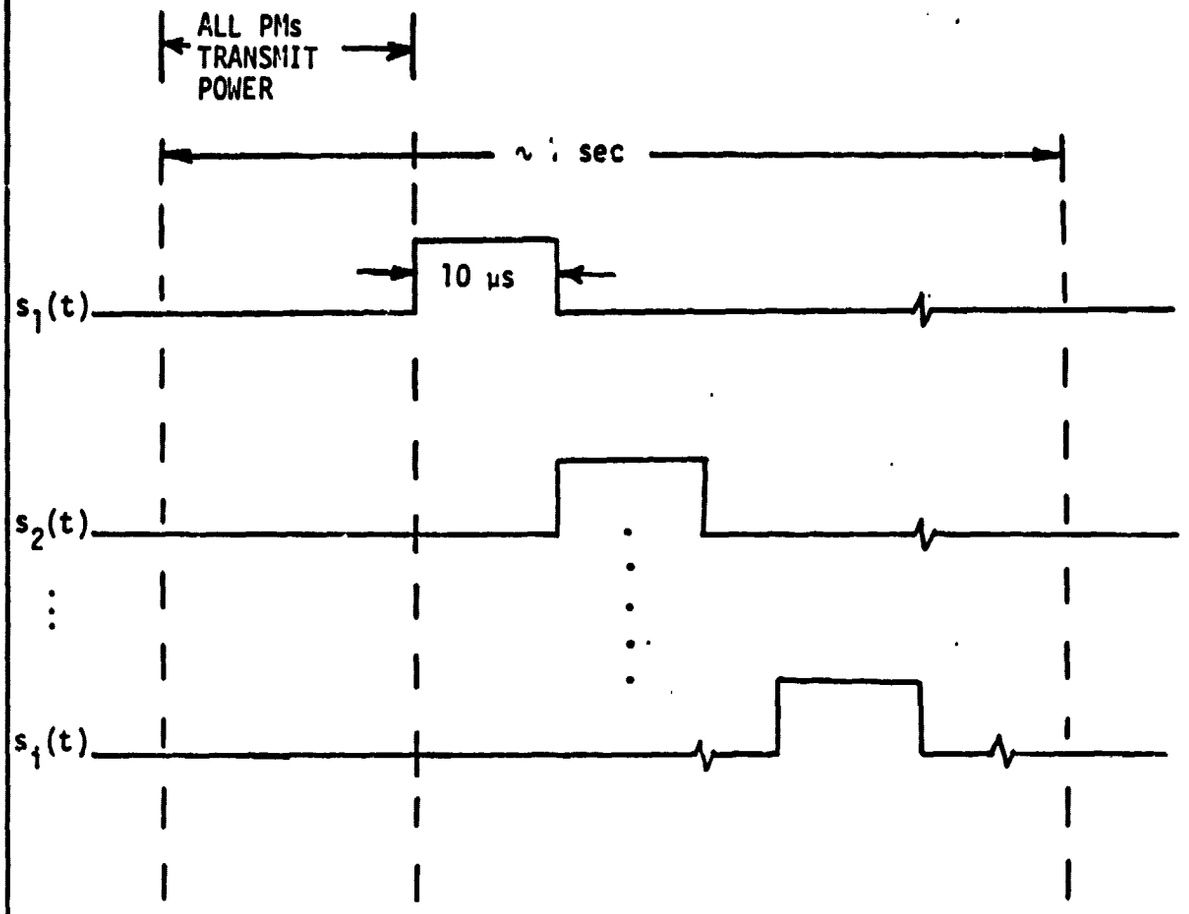

Figure 3.10. Sync Waveforms for Four-Tone Scheme.

4.0 RECOMMENDATION FOR BASELINE SPS GROUND BASED PHASE CONTROL SYSTEM

The results presented in the previous two sections will be combined and used to recommend a baseline for the ground based phase control system. The functional block diagram of such a system is depicted in Fig. 4.1. We also show the system timing hierarchy in the same diagram. Essentially, all subsystem timing and frequency generation are synchronized (at least in frequency) to the frequency standard on board the spacetenna. This approach simplifies considerably the design of the subsystems and eliminates the adverse effect of the long term drift of the frequency reference on system performance. In what follows, we shall descirbe qualitatively the operation of this baseline system. A detailed description of critical subsystems are also presented.

4.1 Functional Description of the SPS Ground Based Phase Control System

A 5 MHz cesium primary standard is used on board SPS to drive a Master Frequency Synthesizer (MFS) as shown in Fig. 4.1. There are two outputs from the MFS. The first is a reference frequency at 490 MHz. This frequency is to be multiplied up to the carrier frequency at the pilot transmitter and at each power module. The 490 MHz IF is chosen to minimize the attenuation loss caused by the length of the cables running from the MFS to the subsystems. The other signal is a data clock with a period equal to approximately 101,552 cycle/sec. Its purpose is to synchronize the time division multiplexed (TDM) operation modes of the PMs.

The 490 MHz reference is multiplied up to 4900 MHz (or any other convenient multiplies of 490 MHz) at the downlink pilot transmitter end.

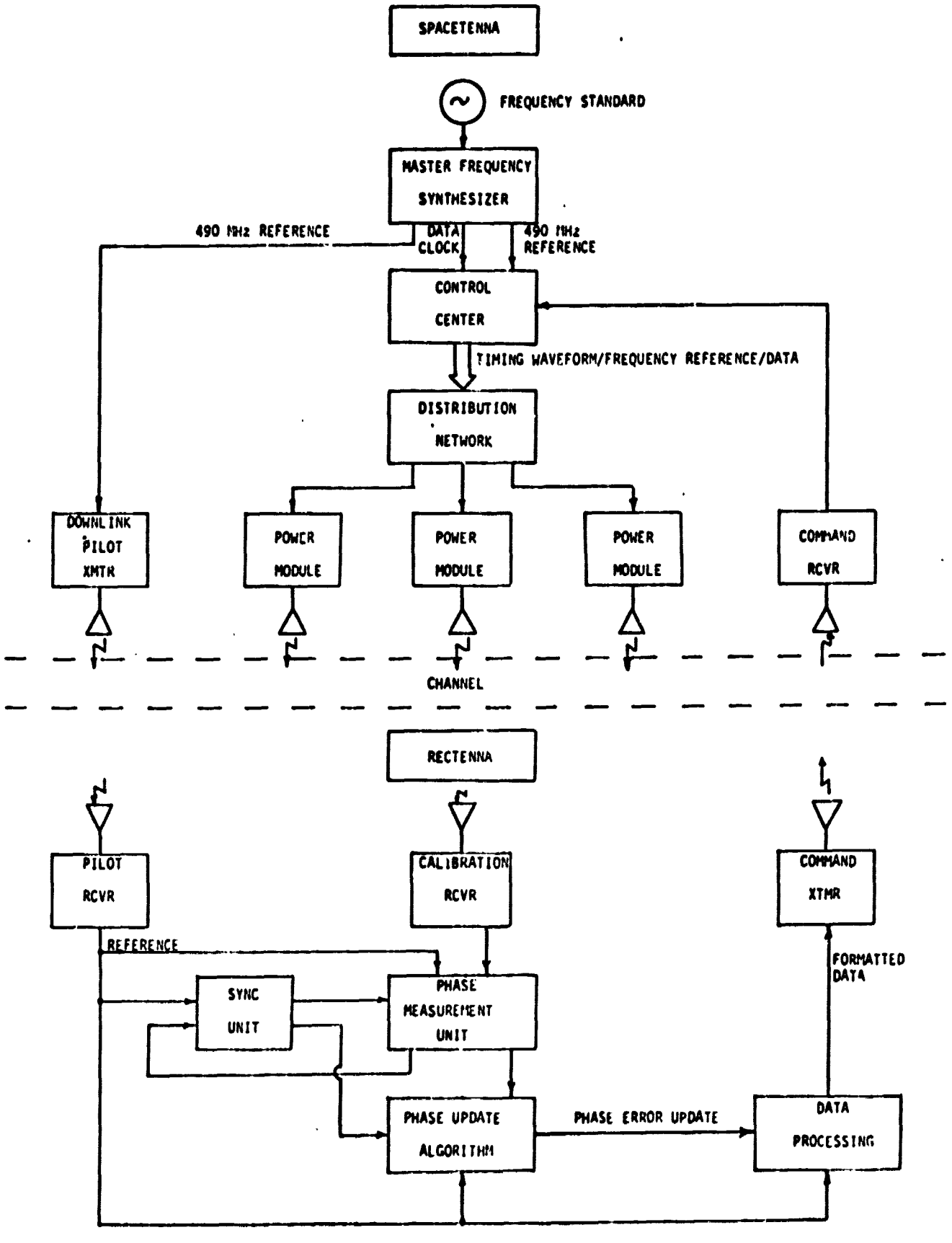

Figure 4.1. SPS Ground Based Phase Control Functional Block Diagram Showing System Timing Hierarchy.

80 0058

This pilot is received on the ground and serves as the ground frequency reference.

The control center on board SPS processes its inputs and distributes the control signals to the PMs via a distribution network. The control center accepts two groups of inputs. First, there is the phase update data demodulated by the command receiver. The control center takes this data and processes them into a form suitable for distribution to control the phases of the PMs. The other is the system timing and frequency reference signals from the MFS. They are used for system synchronization purposes.

The PM operates in three modes: (1) power mode, (2) measurement mode and (3) ambiguity resolution mode. These modes are controlled by the control center. The control center also adjusts the phases of the individual power beams continuously via 10 bit digital phase shifters at 2.45 GHz. Most of the time, the PM will be in a power mode (mode 1) in which a tone at 2.45 GHz is delivered to the subarray antenna. For once (10 μsec) every sec, the PM will be switched to the calibration mode, i.e., either mode 2 or 3. In that case, the carrier will be modulated by square waves coherent with the carrier. The resultant transmitted waveform will have components with frequency offsets from the (suppressed) carrier equal to odd multiples of the frequency of the square wave. This method of generating sidetones using a constant envelope signal avoids the problems associated with the nonlinear amplitude induced phase distortions (AM/PM) introduced by the klystron. The output power level,however, is degraded by approximately 4 dB since other harmonics are also generated.

On the ground, the calibration receiver is tuned to the sidetone frequencies (mode 2 and mode 3 signals). At the phase measurement unit,

the phases of the sidetones are measured against the ground reference. These phases are inputs to the phase update algorithm. A byproduct of the phase measurement unit is the signal power level. It is used to derive synchronization information in the sync unit. The phase error estimates computed by the update algorithm are then processed and formatted. The command transmitter is responsible for relaying the phase update data to the satellite.

4.2 Pilot Transmitter and Power Modules

At the pilot transmitter (see Fig. 4.2), the 490 MHz reference is multiplied up to 4.9 GHz. It is transmitted down to the ground to establish a constant ground frequency reference. Since both the pilot reference and the downlink measurement signal see the same Doppler due to the relative motion between the satellite and the ground receiver, the effect of Doppler cancels itself out when the signal phase is measured against the pilot reference.

Each power module is connected to the control center through a distribution network. At the power module, the 490 MHz reference is multiplied up to S-band. The phase of this signal is continuously corrected by a 10 bit digital phase shifter whose value is set by the control center. The S-band signal is also divided down and hardlimited to generate square waves. In this way, the square waves are coherent with the S-band reference. A switch controlled by the monitor and control signals from the Control Center is used to select the appropriate waveforms to be mixed with the carrier. In mode 1, the square waves are suppressed. In mode 2, the 19.14 MHz square wave is used. Finally, the 9.57 MHz square wave is used for mode 3. Since the effect of mixing these waveforms is equivalent to biphase modulate the carrier,

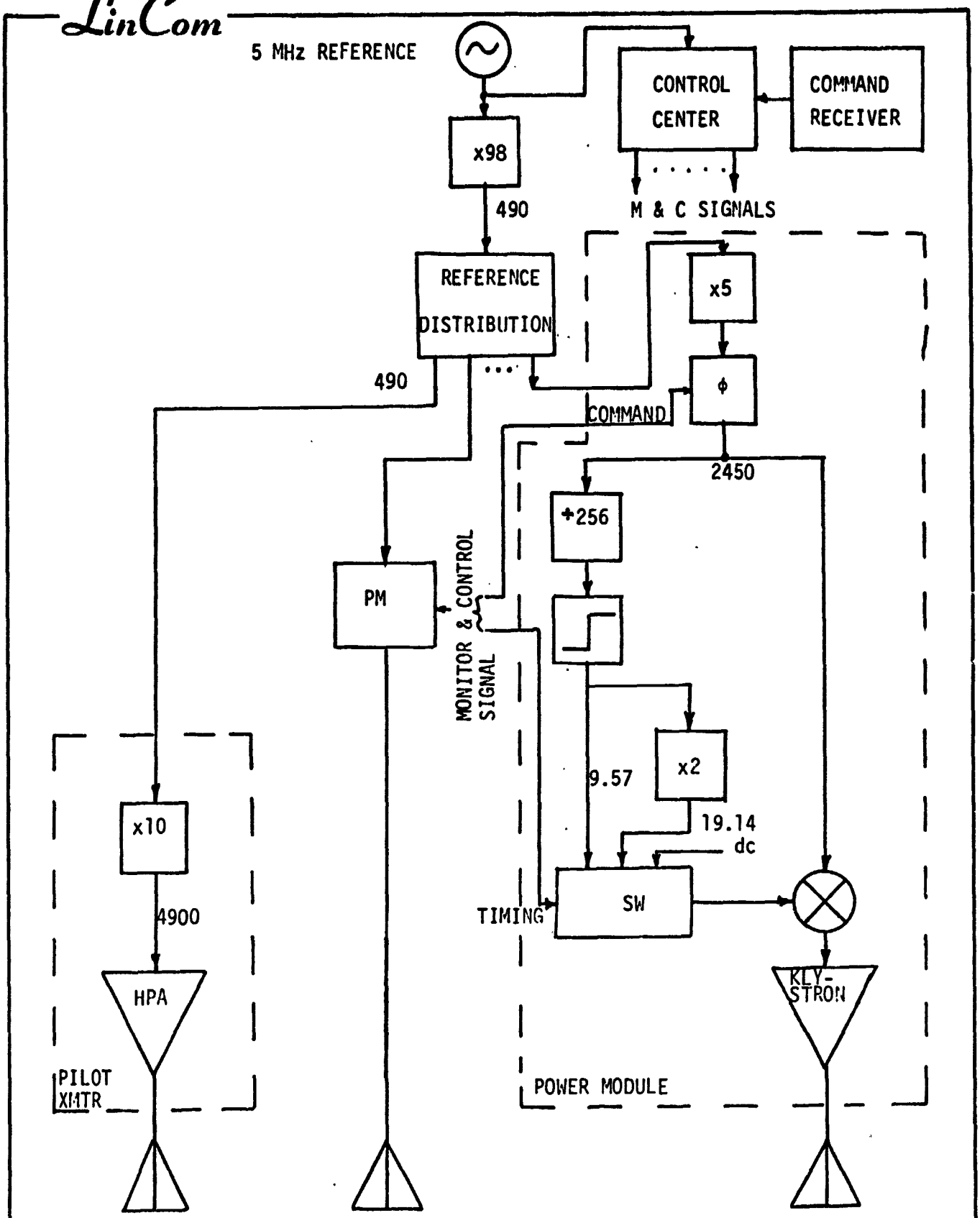

Figure 4.2. Pilot Transmitter and Power Module on Board SPS.

there is no variation in the amplitude of the carrier. As a result, all three modes will generate the same amount of phase shift due to AM/PM conversions introduced by the klystron amplifier.

The scheme above assumes that the measurement and ambiguity resolution modes are time division multiplexed. It is also possible to generate the measurement and ambiguity resolution waveforms at the same time, at a greater power loss penalty. A simple way to generate the combined waveforms is given in Fig. 4.3. The modification on the overall system is minimal if this approach is used and we shall not pursue it any further.

4.3 Pilot Receiver, Calibration Receiver and Measurement Unit

The 4.9 GHz downlink pilot signal is tracked by a phase locked loop on the ground (see Fig. 4.4). The loop is designed with a bandwidth to track out the effect of satellite motion induced Doppler (radial velocity 300 cm/s maximum). The VCO quiescent frequency is selected to be 490 MHz. The output of the VCO is also used as a ground timing reference. The 490 MHz signal is processed to provide 4 different reference tones at 70 ± 9.57 and 70 ± 19.14 MHz for the measurement unit. The way that these tones are generated is very similar to the generation of squarewave modulated signals in the PMs on the spacetenna. The resultant tones are all coherently related to the 490 MHz reference. A convenient IF of 70 MHz is obtained by down-converting the S-band signal with a local oscillator multiplied up to 2.38 GHz.

The received calibration signal at the center frequency of 2.45 GHz is first notch filtered to suppress the interference from the downlink power beam. One requirement is to insure that the front end low noise

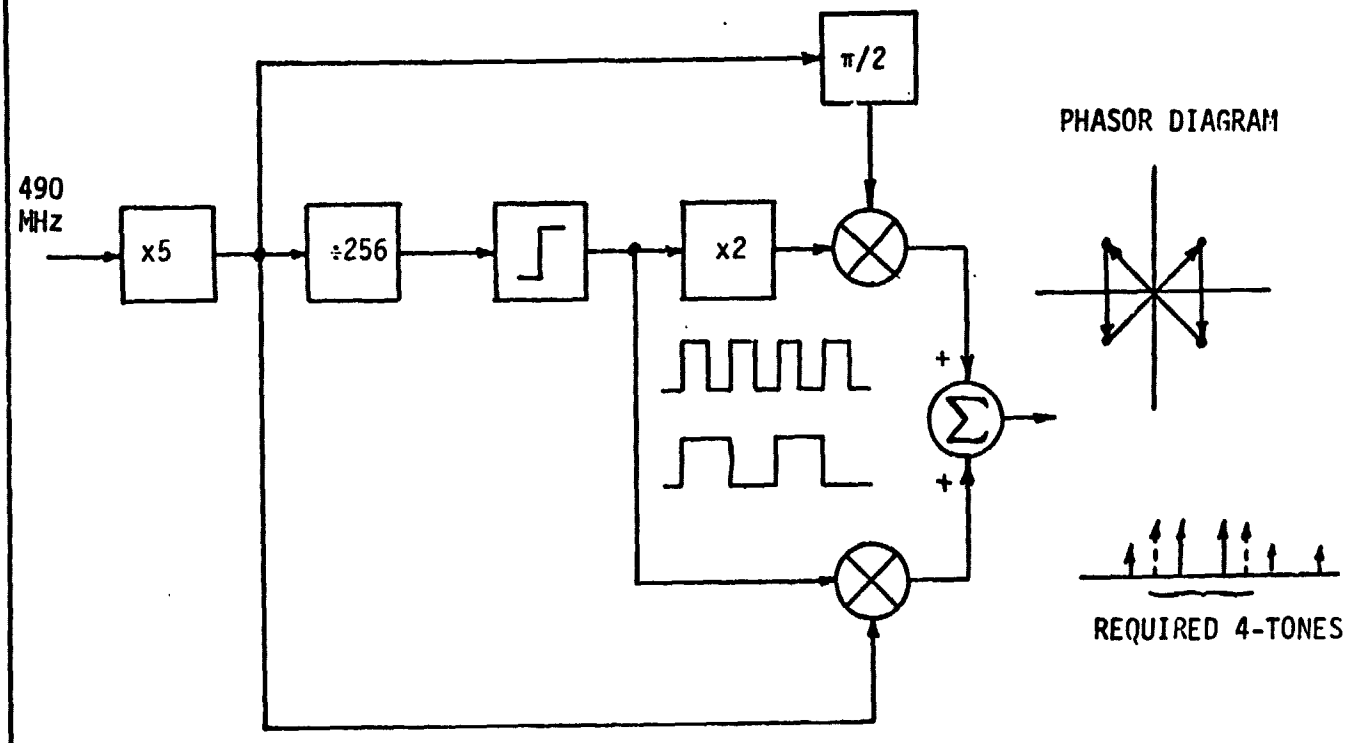

Figure 4.3. Simultaneously Generation of 4 Sidetones.

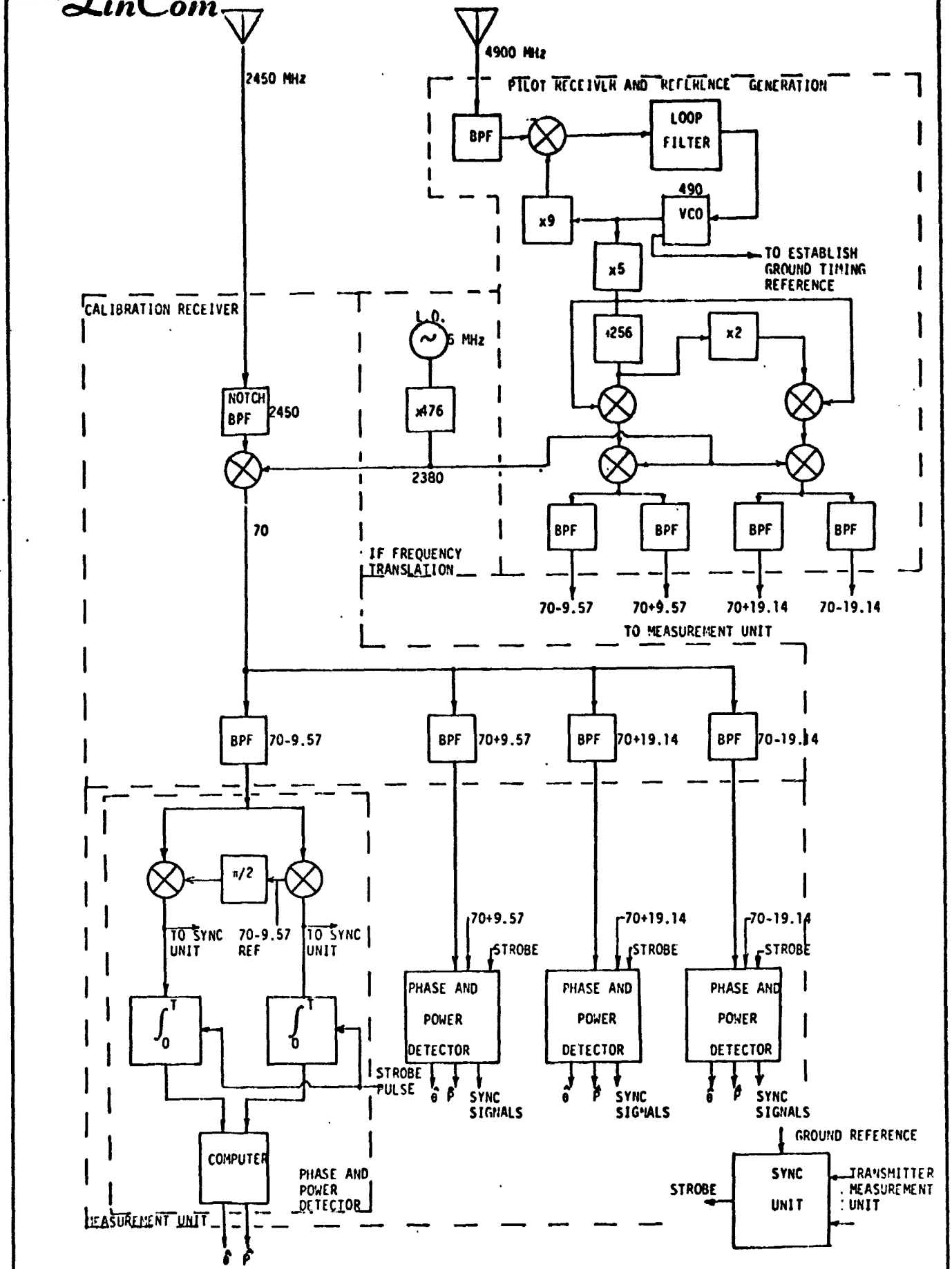

Figure 4.4. The Pilot and Calibration Receiver.

amplifier (not shown in the diagram) is not saturated by the power leakage. The signal is then down converted to an IF of 70 MHz, using the same LO source as the pilot reference. After the mixer, the signal is split and filtered. They are separated into four received tones at 70 $\pm$ 9.57 and 70 $\pm$ 19.14 MHz. Depending on the mode of operation, three distinct cases can happen: (1) there is no signal present in any of the four frequencies, (2) signal present at 70 $\pm$ 9.57 MHz only, and (3) signal present at 70 $\pm$ 19.57 MHz only. The detection of these cases provide the sync unit with the necessary inputs.

Each of these outputs are connected to a measurement unit. The signal is split into two paths, each of which is mixed with the I and Q versions of the reference at the same frequency. The output of the mixers provide the inphase and the quadrature projections of the phase difference between the incoming signal and the reference. They are integrated over the 10 μsec interval for improved signal to noise ratio and at the end of the allocated time slot, they are sampled and dumped to a computer. The computer is simply a device to determine the signal phase and power level. For example, we can use $\theta = \tan^{-1}(A \sin \theta / A \cos \theta)$ and $P = \frac{1}{2}[(A \sin \theta)^2 + (A \cos \theta)^2]$ where θ is the phase difference, A is the amplitude and P is the power level, provided that $A \sin \theta$ and $A \cos \theta$ are the outputs of the integrate and dump circuit. The estimates θ and P can now be used in the update algorithm and the sync unit. Note that the raw data for the I and Q phase components before the integrate and dump filters are also extracted for synchronization purposes.

4.4 System Synchronization

There are three levels of synchronization requirements for a ground

based phase control system. First of all, we need to synchronize to the switching of the time slots allocated to different PMs. This is analogous to symbol synchronization in a data transmission system. After this is done, we need to differentiate the time slot that a particular PM is allocated to. This is analogous to frame synchronization in a TDMA operation. Finally, we have to be able to tell whether the system is in a measurement or an ambiguity resolution mode.

In Fig. 4.5, we show the start-up waveform which is capable of providing "symbol" and "frame" sync. Each frame of 1 sec duration is divided into 101,552 + 2 slots. The first two slots are the sync slot in which all PMs transmit only the carrier. It serves to indicate the start of the frame. The following slots are occupied by the PMs assuming the measurement mode in a sequential order. The odd numbered PMs transmit at $\pm$9.57 MHz and the even numbered PMs transmit at $\pm$19.14 MHz. The received waveform on the ground is summarized in Fig. 4.5. To establish symbol sync, the received waveform is tracked by an early-late type bit sync loop given in Fig. 4.6. The error signal is generated by integrating the repetitive on-off signal over one symbol time centered around the transitions. Both signals from $\pm$9.57 and $\pm$19.14 MHz are used and their appropriate contributions are weighed by the gains G_1 and G_2. The start-up waveforms are transmitted for a few seconds until the bit sync is in lock and the control center on board SPS then switches the PMs to the normal calibration mode.

After initialization, the waveforms are scheduled into a calibration cycle as shown in Fig. 4.7. In a calibration cycle, all but one frame (1 sec) is devoted to the measurement mode. The last frame is devoted to ambiguity resolution. The arrangement maximizes

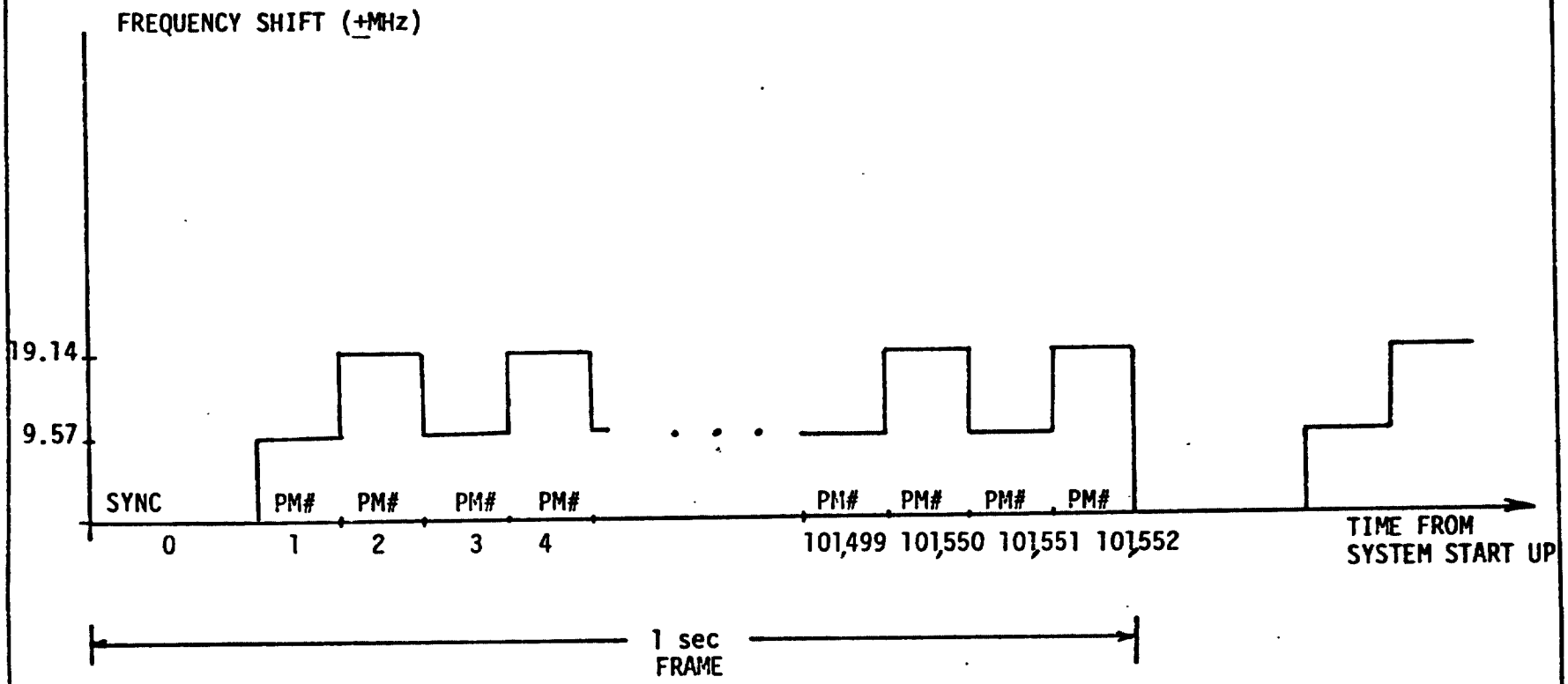

Figure 4.5. Start Up Waveform.

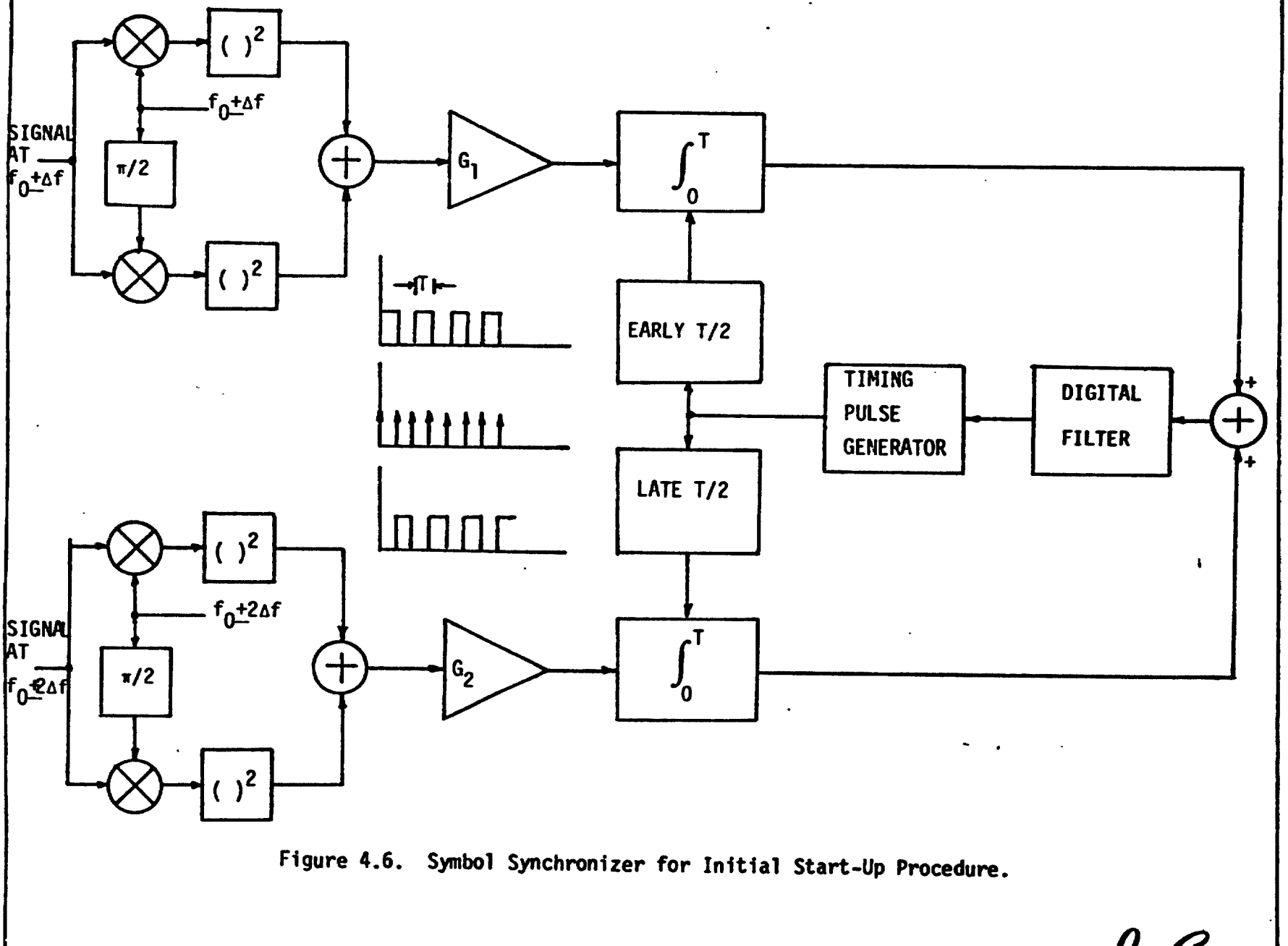

Figure 4.6. Symbol Synchronizer for Initial Start-Up Procedure.

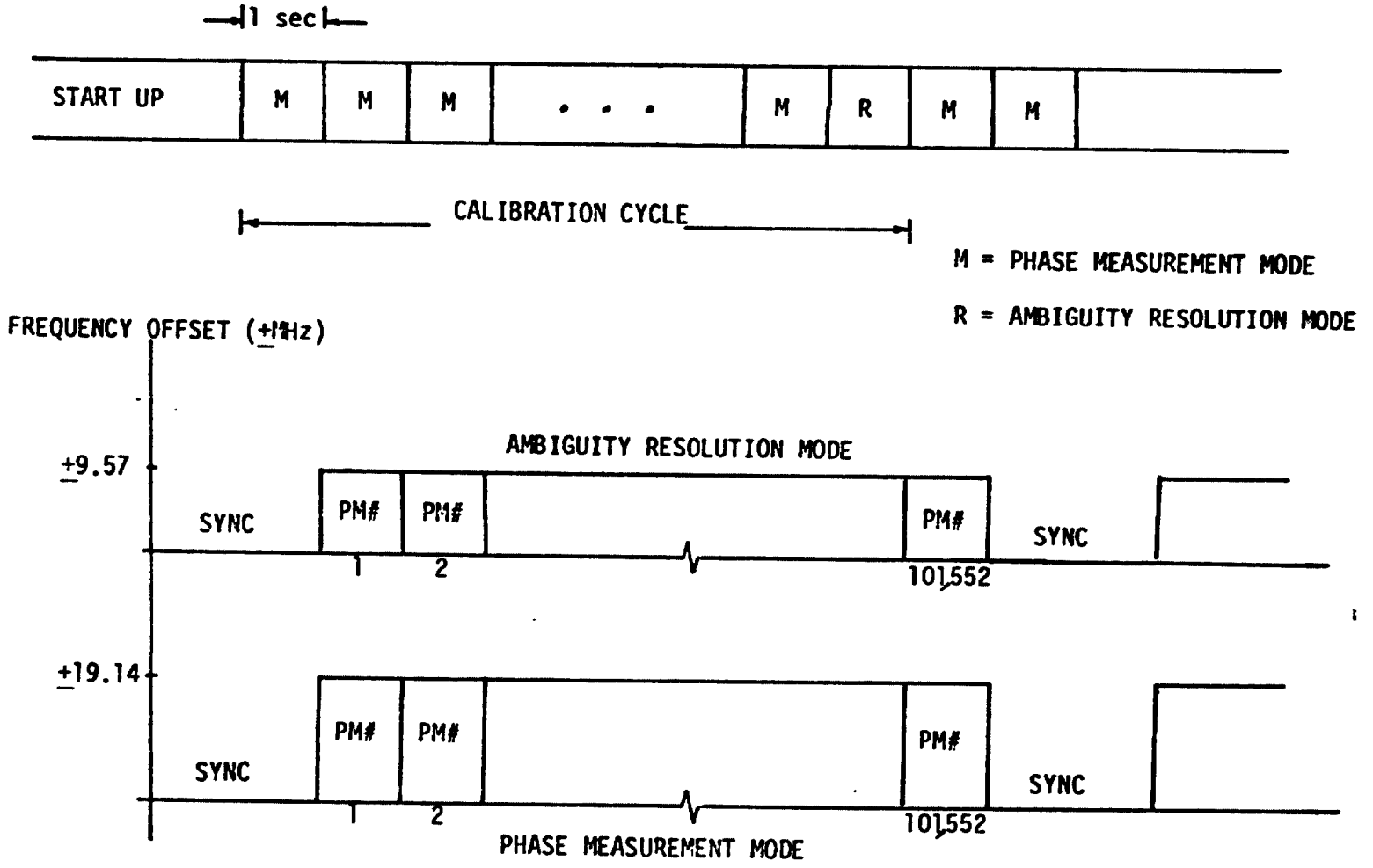

Figure 4.7. Timing Diagram for Measurement and Ambiguity Resolution on Normal Operation.

the utilization of the available calibration time since the phase ambiguity need only be resolved once in an ideal situation. The frequencies used in each mode are also depicted in Fig. 4.7. The SYNC slot is required to periodically correct the bit sync. (At this time, the bit sync only looks at the sync slot transitions.) The two modes are easily distinguished by inspecting the power level at the appropriate frequencies.

REFERENCES

[1] Lindsey, W.C., "A Solar Power Satellite Transmission System Incorporating Automatic Beam Forming, Steering and Phase Control," prepared for NASA JSC, June, 1978, LinCom Corporation, Pasadena, CA.

[2] Orbit Data supplied by Lou Livingston, LEC, April, 1979.

[3] Lawrence, R. S., et al., "A Survey of Ionospheric Effects Upon Earth-Space Radio Propagation," Proc. IEEE, vol. 52, pp. 4-27, January 1964.